JOURNAL OF GEOPHYSICAL RESEARCH, VOL. 94, NO. B10, PAGES 14,111-14,125, OCTOBER 10, 1989

Magnetotelluric Observations Across the Juan de Fuca Subduction System in the EMSLAB Project

PHILIP E. WANNAMAKER,[1] JOHN R. BOOKER, JEAN H. FILLOUX, ALAN G. JONES, GEORGE R. JIRACEK, ALAN D. CHAVE, PASCAL TARITS, HARVE S. WAFF, GARY D. EGBERT, CHARLES T. YOUNG, JOHN A. STODT, MARIO MARTINEZ G., LAWRIE K. LAW, TAKESI YUKUTAKE, JIRO S. SEGAWA, ANTHONY WHITE, AND A. W. GREEN, JR.

A magnetotelluric (MT) transect has been obtained near latitude 45°N from the active Juan de Fuca spreading center, across the subduction zone and Cascades volcanic arc, and into the back arc Deschutes Basin region. This paper presents the MT data set and describes its major characteristics as they pertain to the resistivity of the subduction system. In addition, we discuss the measurement and processing procedures employed as well as important concerns in data interpretation. Broadband audiomagnetotelluric (AMT)/MT soundings (approx. 0.01-500 s period) were collected on land with considerable redundancy in site location, and from which 39 sites were selected which constrain upper crustal heterogeneity but sense also into the upper mantle. Fifteen long-period MT recordings (about 50-10,000 s) on land confirm the broadband responses in their common period range and extend the depths of exploration to hundreds of kilometers. On the Juan de Fuca plate offshore, 33 out of 39 sea floor instruments at 19 locations gave good results. Of these locations, five magnetotelluric soundings plus two additional geomagnetic variation sites, covering the period range 200-10^5 s approximately, constitute the ocean bottom segment of our profile. The feature of the land observations which probably relates most closely to the subduction process is a peak in the impedance phase of the transverse magnetic mode around 30-50 s period. This phase anomaly, with a corresponding inflection in the apparent resistivity, is continuous eastward from the seacoast and ends abruptly at the High Cascades. It signifies an electrically conductive layer in otherwise resistive lower crust or upper mantle, with the layer conductance decreasing eastward from the coast to a minimum under the Coast Range but increasing suddenly to the east of the central Willamette Basin. The higher conductance to the east is corroborated by the vertical magnetic field transfer function whose real component shows negative values in the period range 100-1000 s over the same distance. The transverse electric mode apparent resistivity and phase on the land display a variety of three-dimensional effects which make their interpretation difficult. Conversely, both modes of the ocean floor soundings exhibit a smooth progression laterally from the coastal area to the spreading ridge, indicating that the measurements here are reflecting primarily the large-scale tectonic structures of interest and are little disturbed by small near-surface inhomogeneities. The impedance data near the ridge are strongly suggestive of a low-resistivity asthenosphere beneath resistive Juan de Fuca plate lithosphere. Approaching the coastline to the east, both impedance and vertical magnetic field responses appear increasingly affected by a thick wedge of deposited and accreted sediments and by the thinning of the seawater.

INTRODUCTION

Our goal in acquiring magnetotelluric measurements is to increase understanding of the physicochemical state of the Earth's interior through its influence on the electrical resistivity. Generation and subduction of the lithosphere are among the most fundamental processes shaping the earth and, for investigation by induction researchers in North America, the Juan de Fuca system is fortuitously close at hand. Consequently, we have collected a profile of tensor magnetotelluric (MT) soundings trending approximately east-west and located near the center of the EMSLAB magnetovariation array (Figure 1) [*EMSLAB Group*, 1988; *Gough et al.*, this issue]. Because the profile crosses the northern Oregon coast near the town of Lincoln City, it is referred to as the Lincoln Line. The measurements are intended to yield a detailed resistivity cross section from the Juan de Fuca spreading ridge through the subduction complex, the Willamette Basin, the Cascades volcanic arc, and into the back arc Deschutes Basin region. Consideration of the electric field with the magnetic in the MT method (i.e., measuring the plane wave impedance of the Earth) increases our resolution of buried structure, especially layerlike geometries, over using the magnetic field alone. This also makes interpretation more difficult, however, because the electric field can be strongly influenced by shallow crustal structures which are not our primary targets of investigation.

The landward segment of the profile (Figure 2) consists of 39 selected broadband AMT/MT observations (approximately 0.01-500 s period) augmented by 15 long-period MT recordings (about 50-10,000 s). A purpose of the broadband soundings is to account for the effects of upper crustal lateral heterogeneity, but such soundings also sense through the crust and well into the upper mantle. The long-period MT data confirm, but are generally of higher quality than, the broadband responses in their common period range and extend the depths of exploration to hundreds of kilometers. On the sea floor portion of the profile (Figure 1) [*EMSLAB Group*, 1988], we have five MT soundings plus two additional magnetovariation sites which collected data over the period range 200 s to approximately 10^5 s. The coarser site spacing relative to the land in part is dictated by

[1]The affiliations of the authors may be found on the last page of this paper.

Paper number 89JB00680.
0148-0227/89/89JB-00680$05.00

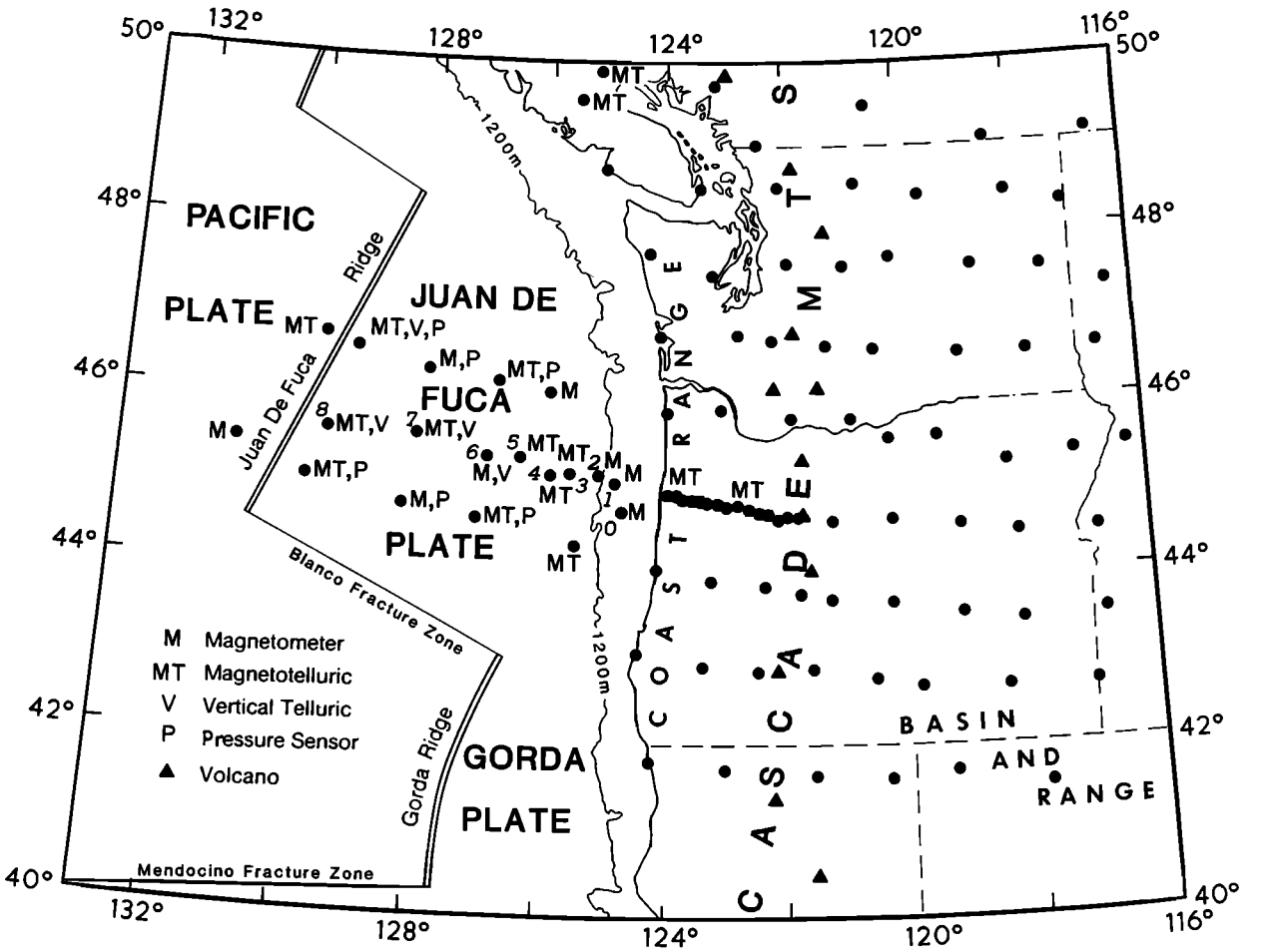

Fig. 1. Instrument locations of entire EMSLAB array. On land, the unlabeled dots indicate locations of three-component magnetovariometers. The E-W trending concentration of dots in northwestern Oregon denotes the long-period MT recorders along the land portion of the Lincoln Line. Seafloor array sites are labeled according to instrument type and sites 0 through 8 are given for the sea floor extension of the Lincoln Line. No data was recovered from sea floor sites 0 and 6.

the much greater expense of instrument deployment by ship but more importantly reflects the much greater uniformity of the near-surface geologic structure on the sea floor. Results at periods shorter than about 200 s inevitably are lacking in ocean bottom MT because the magnetic signals especially are attenuated by the overlying conductive seawater. The primary purposes of this paper are to present the measurements taken by the numerous researchers involved as a unified, coherent data set and to describe major characteristics of the data as they pertain to the resistivity of the Juan de Fuca subduction system. In addition, we discuss the measurement and processing procedures employed as well as important concerns in data interpretation. Several papers on interpretation follow this one which make use of all or part of the Lincoln Line data set.

A brief review of MT theory is given here primarily to define terms and conventions. The concepts introduced provide a foundation for the detailed discussion of our observations which follows. We then describe the measurement and processing techniques employed by the researchers who gathered data along our profile. This should indicate the difficulty of the measurements we make and the rigor of the methods required to achieve good results.

Source Fields and Tensor Relationships

The MT method makes use of naturally-occurring electromagnetic (EM) fields as sources for exploring subsurface resistivity structure [*Vozoff*, 1986]. Usually, the remote origin of the natural fields together with the very high index of refraction of the Earth relative to the air allows us to treat the incident vector electric ($\vec{E}$) and magnetic ($\vec{H}$) fields as planar and propagating vertically downward into the ground [but see *Egbert and Booker*, this issue]. Owing to the dominance of conduction over dielectric displacement for the range of resistivities and periods of interest, the propagation of EM fields in the earth is diffusive. The amplitudes of the electric and corresponding orthogonal magnetic vectors of a plane wave entering a uniform conducting half-space decrease by 1/e over a distance called the skin depth, $\delta \simeq 503\sqrt{\rho T}$ in meters, where ρ is the resistivity (inverse of conductivity σ) in ohm meters and T is the period in seconds. We see here that the downgoing incident fields can reach the deeper structures and be scattered back with significant amplitude for measurement, only at the longer periods. This ability of MT to discriminate in depth holds fundamentally even for

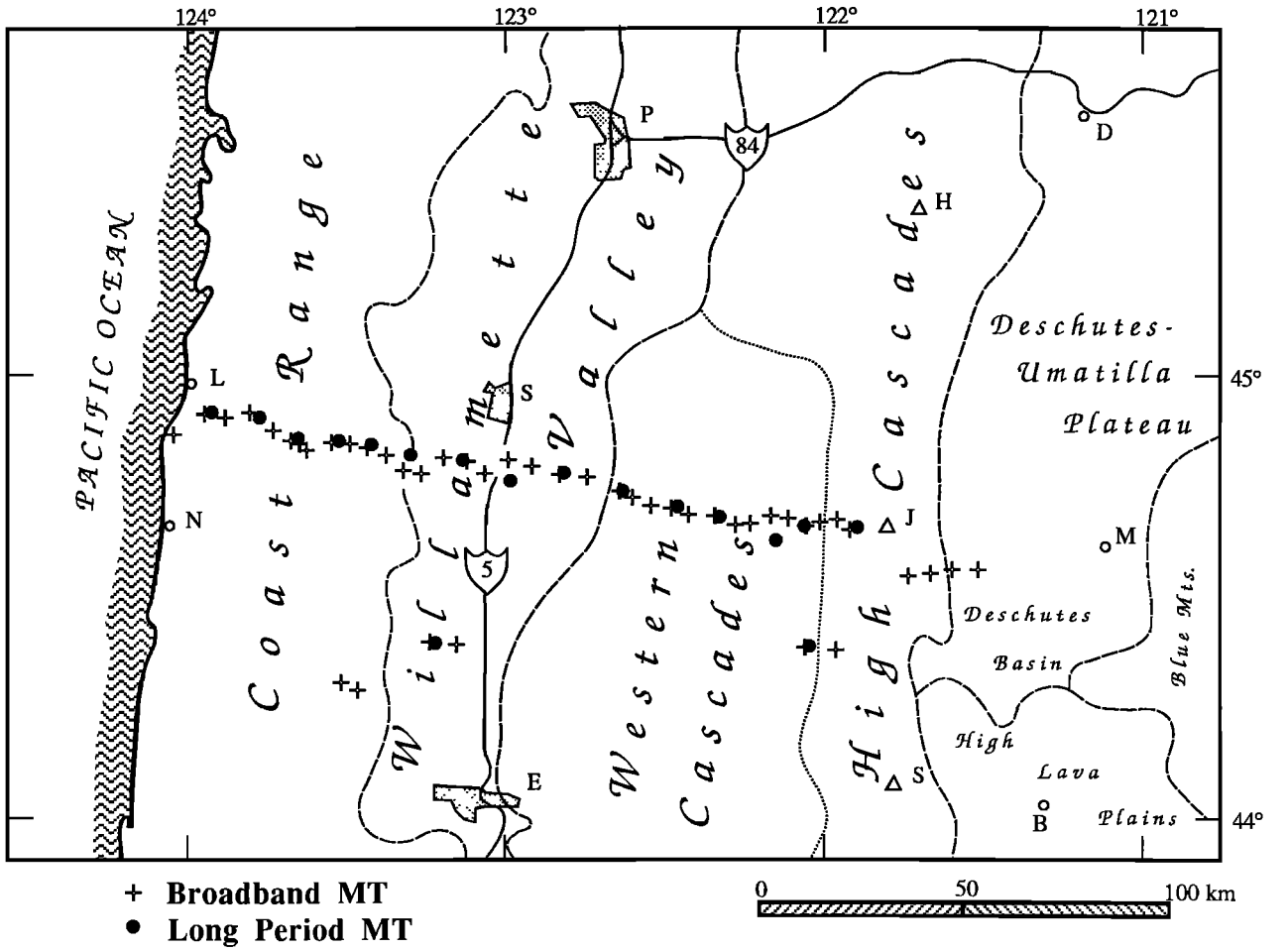

Fig. 2. Broadband and long-period magnetotelluric soundings along the landward portion of the Lincoln Line and also along the mini-EMSLAB test traverse farther south [*Young et al.*, 1988]. Urban areas include Portland (P), Salem (S), Eugene (E), Newport (N), Lincoln City (L), Bend (B), Madras (M), and The Dalles (D). Cascades volcanoes are labeled as triangles: Mount Hood (H), Mount Jefferson (J), and South Sister (S).

complex natural settings, although often the effects of shallow structures may persist in the data from short through long periods (see discussion of observed MT responses).

The secondary or anomalous EM fields induced around a three-dimensional structure in general may be polarized arbitrarily with respect to the incident fields. Therefore, the relation between the total ($\vec{E}$) and ($\vec{H}$) at the surface for a plane wave source must be expressed by a complex-valued tensor impedance, i.e.,

$$\begin{bmatrix} E_x \\ E_y \end{bmatrix} = \begin{bmatrix} Z_{xx} & Z_{xy} \\ Z_{yx} & Z_{yy} \end{bmatrix} \begin{bmatrix} H_x \\ H_y \end{bmatrix} \tag{1}$$

which can vary with period, from sounding to sounding, and with orientation of the x-y coordinates. Similarly, the relationship

$$[H_z] = [M_{zx} \; M_{zy}] \begin{bmatrix} H_x \\ H_y \end{bmatrix} \tag{2}$$

can be defined for the vertical magnetic field. A right-handed coordinate system with z positive down is assumed. With field data, one often rotates the original x-y coordinates mathematically to extremize the tensor elements and thereby obtain estimates of geoelectric strike [*Word et al.*, 1971]. In natural three-dimensional settings, however, the principal direction or strike resulting from the impedance may vary independently from that due to H_z, with both period and location.

Rather than work directly with the impedance elements as they appear in (1), we instead construct simple functions from each. One useful function is apparent resistivity, generically denoted by ρ_a, and defined from the element magnitudes in (1). Specifically, from Z_{xy}, for instance, it is

$$\rho_{xy} = \frac{1}{\omega \mu_0} |Z_{xy}|^2 \tag{3}$$

in units of ohm meters, where $\omega = 2\pi/T$ is radian frequency and μ_0 is the magnetic permeability of free space. This operation when applied to the impedance on a uniform half-space returns the intrinsic resistivity ρ. For more complicated geometries, ρ_a versus T usually resembles a smoothed version of the true resistivity over increasing distances below the measurement site. It is common practice to substitute measured apparent resistivity values into the

previous formula for skin depth to obtain crude estimates of depth to structure. Complementary to the apparent resistivity is the phase of the impedance, e.g., ϕ_{xy}. Over a uniform half-space of any resistivity, ϕ_{xy} is 45°. Parenthetically, ϕ_{yx} in this case is -135° due to the right-handed coordinate system, but we generally rotate this phase to the first quadrant for display and interpretation. Over any one-dimensional earth, a Hilbert transform relationship between the apparent resistivity and the impedance phase can be proven [*Boehl et al.*, 1977]. This proportionality between the impedance phase and the slope of the apparent resistivity versus T is observed almost invariably over heterogeneous earths as well. A similar Hilbert transform relation between the real and imaginary components of M_{zx} and M_{zy} is usually observed in keeping with the approximately causal nature of the linear system (2).

The structure of the tensor relations (1) and (2) simplifies for special cases of resistivity structure. Over a two-dimensional earth, elements Z_{xx}, Z_{yy} and M_{zx} vanish if the x and y axes are aligned with and across strike respectively (the principal directions). This constitutes a decoupling of the total fields into two independent modes: the transverse electric (TE, or E-polarization with E_x, H_y, H_z) and the transverse magnetic (TM, or B-polarization with H_x, E_y, E_z). In other words, the TE mode comprises electric fields (currents) parallel to strike while the TM mode comprises electric fields (currents) perpendicular to strike. Since we could carry out only a single well-sampled profile of MT soundings in EMSLAB, we must derive meaningful resistivity models using primarily a two-dimensional analysis [see *Wannamaker et al.*, this issue; *Jiracek et al.*, this issue]. To facilitate two-dimensional modeling, the Lincoln Line was designed to cross tectonic units, including both upper crustal structure and the subduction system, whose preferred orientation appeared predominantly N-S.

Equations (1) and (2) reduce much further when considering just one-dimensional geometries. Now, the polarization of the incident EM fields is immaterial so that $Z_{xy} = -Z_{yx} = Z_{1D}$, which is the scalar impedance of the one-dimensional earth, while Z_{xx}, Z_{yy} and H_z all equal zero. One-dimensional conductivity models of individual MT soundings are very popular because the algorithms fit easily on desktop computers, but these models frequently are suspect due to common departures from one-dimensionality in nature. They can be valuable in constructing initial guesses for subsequent two-dimensional modeling [*Waff et al.*, 1988, *Livelybrooks et al.*, this issue; *Young and Kitchen*, this issue].

Measurement and Processing Techniques

A minimum of five channels of electromagnetic time series (E_x, E_y, H_x, H_y, H_z) need to be collected at a survey site in order to estimate the MT transfer functions (1) and (2). Of foremost importance, the natural fields we measure are very low in strength; full-scale temporal variations of only about a nanotesla for $B=\mu_0 H$ and a microvolt per meter for E are typical. The signal spectrum moreover is far from white with strengths in the so-called mid or dead band (0.2-20 s approximately) often 10-100 times weaker than at periods above or below. Sources of electromagnetic noise on land which can rival or overwhelm the signal and so degrade our estimates include man-made or cultural interference, electronic sensor and amplifier noise, chemical instability in the E field electrodes, vibration, and thermal drift [*Clarke et al.*, 1983]. Cultural noise and thermal drift presumably are not serious on the ocean bottom but attenuation especially of the magnetic field signals by the overlying seawater prevents collection of MT data at periods shorter than a few minutes [*Filloux*, 1987]. Sources of noise notwithstanding, the MT fields we measure also depart sometimes from the assumption of a plane wave geometry [*Egbert and Booker*, this issue]. Such departures occur toward long periods due to solar-magnetic storms in the magnetosphere and ionosphere but also at periods even less than 1 s during times of nearby thunderstorm activity. These characteristics of the measurement problem necessitate ultra low-noise sensors and signal conditioning plus sophisticated time series processing. Relevant features of the individual recording instruments used in EMSLAB are summarized in Table 1 and explained in more detail below.

The electric fields invariably are obtained as voltage differences over orthogonal grounded bipoles, which terminate in quiet and stable chemical electrodes consisting of a base metal and its salt [*Petiau and Dupis*, 1980]. The combination used most often for the land data was Pb-$PbCl_2$ but good results were obtained also with Cu-$CuSO_4$. To boost the E field signal of the land measurements, bipole lengths on the order of 100 m were laid out. A variety of types of sensor are available for measuring the magnetic field. The broadband AMT/MT instruments in our study mainly utilized large, ferrite-cored induction coils for the three components of $(\vec{B})$ although one system used a cryogenic SQUID. The long-period recorders employed flux gate devices. Two additional channels of horizontal magnetic field were recorded or taken from a neighboring site for use as independent references for noise cancellation in the broadband systems (see below). Output from the electric and magnetic field sensors was fed immediately through high-gain analog amplification and band limiting, usually with custom-built electronics. The broadband systems divided their signal spectrum into at least three overlapping period bands. This was necessary to economize on the volume of time series to be collected and also allowed extra amplification of the weak midband signal. After antialias filtering, the signals were digitized and results stored, sometimes partially processed, on floppy diskettes for the broadband systems or on cassette tape for the long-period recorders. In addition to high sensitivity and complicated in-field processing capability, it was essential that all MT systems were sturdily constructed to withstand adverse weather, dust, and mechanical shock during transport and deployment. Also, the long-period MT systems had to be securely concealed to prevent theft or vandalism during their approximately 2-month duration of recording.

A very thorough discussion of the difficult measurement of sea floor electromagnetic fields is given by *Filloux* [1987]. Electric fields again are obtained as voltage differences over finite bipoles, but for deployment from ships, it is compelling logistically to use rigid bipoles of short length (6.4 m typically and in EMSLAB). The length must be sufficient however to escape perturbations of the electric field in the vicinity of the instrument case. These arise from possible electronic leakage currents and electrochemical reaction between the case and the seawater, and because the case itself constitutes a resistive inhomogeneity in the

TABLE 1. Summary of Attributes of Magnetotelluric Recording Systems Used in the EMSLAB Project

	Broadband Land				Long Period Land		Seafloor
	Michigan Techical University	University of Oregon	SDSU/CICESE	University of Utah	GSC/Ottawa	University of Washington	Scripps Institution
Manufacture	Phoenix Ltd.	In-house	In-house	In-house	In-house	In-house	In-house
Period range (nominal),s	0.003-1800	0.025-600	0.025-1000	0.008-4000	40-30,000	32-175,000	128-DC
Magnetometer	coils (Phoenix Ltd.)	squid (SHE Corp.)	coils (Geotronics Ltd.)	coils (Geotronics Ltd.)	fluxgates (EDA Ltd.)	fluxgates (EDA Ltd.)	suspended magnets (in-house)
Electrode array	cross (30m bipoles)	L (150 m)	cross (100 m)	cross (100 m)	cross (100 m)	cross (300 m)	cross (6.4 m)
Electrode type	Pb-$PbCl_2$	Pb-$PbCl_2$	Cu-$CuSO_4$	Pb-$PbCl_2$	Pb-$PbCl_2$	Pb-$PbCl_2$	Ag-AgCl
Reference	local (wire link)	local (wire link)	remote (radio link)	local (wire link)	single site	single site	neighboring site
Processing	cascade decimation	FFT	FFT	cascade decimation, coherence sorting	cascade decimation, robust processing	cascade decimation, robust processing	FFT, robust processing
In-field computer	HP 9845B	DEC PDP 11/23	DEC PDP 11/23	DEC PDP 11/23	Datel Ltd. cassette logger	Seadata Ltd. cassette logger	Phillips Ltd. cassette logger

Reference to a company or product name does not imply approval or recommendation of the product by members of EMSLAB or by the agencies who funded the project to the exclusion of other products that may be suitable.

electrically conductive ocean host. An additional design criterion for the ocean floor electric field recording was the ability to measure the long-term field for oceanographic purposes [*Chave et al.*, this issue]. To extract the minute signal from potentially large electrode offset voltages, which themselves may drift in time, the electrochemical offsets were estimated independently by an alternating short-circuiting of the voltage electrodes through a salt-bridge switch or chopper [*Filloux*, 1987]. The H field sensors of four of the sea floor magnetometers on the Lincoln Line were suspended-magnet devices. These have a sensitivity of about 0.2 nT (for B), adequate for long-period field variations, plus the advantage of extremely low power consumption. The other ocean bottom magnetovariation recorders on the Lincoln Line utilized flux gate sensors. Finally, one cannot overstate the extreme care required in fabricating sea floor MT instrumentation to withstand the high-pressure, corrosive, and conductive environment of the ocean bottom [*Filloux*, 1987]. That only one instrument package failed to return at all and that 33 out of 39 instruments in EMSLAB gave good data is a tribute to the growing reliability of long-term EM experiments on the ocean bottom.

Spectral analysis methods used in EMSLAB have been reviewed by *Jones et al.* [this issue] and compared using long-period MT time series gathered for the project. One approach of long standing is simply to apply a fast Fourier transform (FFT) to each channel of EM time series, form cross-power and autopower spectral averages over a finite bandwidth, and compute impedance and vertical field transfer elements from the appropriate spectral combinations [*Sims et al.*, 1971]. More recently, analysis using cascade decimation [*Wight and Bostick*, 1980] has become popular because it allows virtually real-time spectral estimation. Bias errors in the transfer function estimates of the broadband MT data were reduced or eliminated using the aforementioned reference fields, with error bounds calculated accordingly [*Gamble et al.*, 1979a,b]. Most of the broadband systems utilized local reference fields, measured only about 200 m from the base sensors, which worked well in most instances but which sometimes were inadequate in the Willamette Basin area where cultural noise could be correlated over several kilometers distance. Both FFT and cascade decimation approaches have been modified to sort spectra from subsets of the EM time series according to quality and to reject outliers, thereby treating the nonstationary and sometimes nonuniform behavior of the signal and noise [*Stodt*, 1983; *Egbert and Booker*, 1986; *Chave et al.*, 1987; *Chave and Thomson*, this issue]. To ensure consistency in sensor reliability, calibration, and data processing for both broadband and long-period MT systems, a preliminary field test at six sites south of the Lincoln Line was carried out in August 1984 [*Young et al.*, 1988] (Figure 2). Close agreement between the different broadband instruments and with the long-period results in their common period range confirmed that the various land MT systems could yield equivalent data at a particular site on different days.

The sea floor data in particular were processed with a new robust, remote reference algorithm with jackknife error estimates that is described by *Chave and Thomson* [this issue]. The periods of interest for sea floor studies extend to 10^5 s, a decade more than on land. Since there are serious questions about the homogeneity of source fields at very long periods and because it is possible that contaminating electromagnetic fields of variable wavelength induced by ocean motions may be present, a careful study of the behavior of remote reference estimates as a function of the reference type was conducted. Using sea floor site SF3 as the local station, robust remote reference estimates were computed using electric and magnetic references at nearby (SF4) and distant (SF7 and SE3) sea floor sites and magnetic references

from land stations at Victoria, British Columbia, and American Bottom, Oregon. The results show that sea floor electric references produce erratic response functions at short periods (below 1000 s) for nearby reference sites and at long periods (beyond 10^4 s) for distant locations. This is probably due to motional electric fields from gravity waves, and electric references were rejected. Distant land magnetic references produced biased response functions at long periods (greater than 10^4 s), suggesting source field heterogeneity over the 200-1000 km distance separating the measurements. Identical bias effects were seen with distant sea floor sites. By contrast, remote reference estimates using a nearby sea floor magnetometer were essentially identical to conventional single-site results at periods over about 1000 s yet dramatically changed the estimates at short periods where magnetometer noise is expected to increase as the external magnetic field becomes markedly attenuated by the overlying seawater. In most instances, changes of over an order of magnitude in apparent resistivity were observed, and usable responses to periods of about 200 s could be found. Based on these tests, all of the sea floor data were processed using a nearby sea floor magnetic site located at the same geomagnetic latitude for a reference.

OBSERVED MAGNETOTELLURIC RESPONSES

We now present the magnetotelluric measurements gathered along the Lincoln Line. The majority of the data is summarized in the form of pseudosections, where east-west location is the abscissa and log period is the ordinate for contour plots of apparent resistivity, impedance phase and the real and imaginary parts of M_{zy}. Because we have but one profile of concentrated MT observations, and the geologic structures beneath trend approximately N-S, a two-dimensional frame-work will be emphasized here over a full three-dimensional analysis. The measurements therefore will be described in terms of their analogous two-dimensional modes of polarization, with the applicability of a two-dimensional assumption discussed for each mode. Consistent with this, we define the x and y axes to coincide with geographic north and east for all stations and all periods. Following each set of pseudosections, examples of the raw data at several individual MT sites are given to convey the statistical quality of our observations and to substantiate key characteristics of the response as they pertain to earth structure.

The description of the measurements on land is separated somewhat from that of the sea floor observations as the period range and station density of the two data sets are quite different. Values defining the pseudosections of the land data were derived from hand-smoothing (by P. E. W.) of the field sounding curves at the 39 broadband and 15 long-period sites. The broadband soundings used were selected from a total of 73 site occupations from three separate field excursions by the four institutions according to data quality and freedom from local three-dimensional effects. For pseudosection display, we wish to preserve, through the long-period range, the lateral variation in the apparent resistivity as sampled by the more numerous broadband soundings. The smoothed long-period data hence were interpolated linearly to give values at the 39 broadband locations and the resulting long-period apparent resistivities were static-shifted to merge with the broadband values over their common period range (see discussion of static effects below). Overall, the MT response along our profile on land appears adequately sampled because the soundings are isotropic at short periods and tend to group distinctly according to the major geologic features crossed, in particular the upper crustal ones. To define the electrical structure of the Juan de Fuca plate offshore, there are five MT soundings plus two additional geomagnetic variation sites. Sampling demands fortunately appear much lower on the sea floor due to the greater uniformity of geologic conditions at shallow depth. Values from smoothed individual response curves have been used to define pseudosections for the sea floor data also.

Transverse Magnetic Impedance Functions

The observed transverse magnetic quantities ρ_{yx} and ϕ_{yx} will be presented at the outset for two reasons. First, as we will describe, the assumption of a two-dimensional resistivity variation beneath the profile is more immune to common three-dimensional effects for the TM mode data than for the TE. Second, the TM mode appears to exhibit more clearly the effects of resistivity structure related to the Juan de Fuca subduction system.

The TM mode can be complicated to understand due to potentially wide fluctuations of the electric field E_y over sometimes short distances. These fluctuations arise from electric charge distributions originating wherever the field crosses resistivity boundaries [*Price,* 1973; *Jones,* 1983; *Wannamaker et al.,* 1984]. The charge in turn reflects the requirement that electric current across boundaries be continuous. Toward longer periods, the influence of boundary charges around two-dimensional or three-dimensional structures can remain strong but becomes independent of period as the governing Helmholtz equation reduces locally to Poisson's equation. The result is a near-field or static, roughly multiplicative distortion of the impedance which would exist if the structure were not present. Therefore, while deep resistivity variations affect MT observations only at longer periods through the skin-depth concept explained previously, near-surface changes both may figure in the observations at short periods and superimpose their effects upon the impedance to arbitrarily long periods. This situation has lead to repeated calls for the ability to sample the MT response, especially the electric field component, more finely when needed or even to make continuous E field measurements along one's profile [e.g., *Bostick,* 1986].

Fortunately, it is only the impedance magnitude, and hence the apparent resistivity, which is distorted in this manner. As the distortion becomes period-independent, impedance phase anomalies diminish to zero. Small-scale, shallow inhomogeneity consequently affects the phase data only at relatively short periods while larger, deeper bodies affect the phase at longer periods. This very much eases the recognition of deep target structures beneath extraneous surficial clutter. Nevertheless, the apparent resistivity must be incorporated into the modeling process in order to resolve absolute values of crucial parameters like depth and resistivity. To our great advantage, ρ_{yx} and ϕ_{yx} are not very sensitive to variations of the resistivity structure off-line from a profile (three-dimensional effects); it is the boundary charge near to the measurement site which most strongly affects the electric

field and hence the impedance [*Wannamaker et al.*, 1984]. Given the prevailing N-S structural trends beneath the Lincoln Line, we believe that an accurate cross section can result from two-dimensional modeling of the TM mode response [see *Jiracek et al.*, this issue; *Wannamaker et al.*, this issue].

Figure 3 and Plate 1 display the pseudosections of ρ_{yx} and ϕ_{yx} observed along the land portion of the Lincoln Line. (Plate 1 can be found in the separate color section in this issue.) Characteristic of the apparent resistivity pseudosection is a strong vertical orientation of the contours, indicating that several major structural areas have been crossed over the line's 200 km length. The persistence of this orientation to the longest periods is a clear manifestation of boundary charge effects as described above. Porous, water-saturated sediments of the Willamette Basin constitute the most important upper crustal inhomogeneity affecting the data on land. They result in values of ρ_{yx} typically below 10 ohm m throughout nearly the entire period range extending over about the central third of the profile. Moderately higher values ~30 ohm m at short periods) near the middle of the basin correspond to overlying Columbia River basalt flows of Late Tertiary age. Flanking the expression of the Willamette Basin are high apparent resistivities, of the order of 100-1000 ohm m, over the Siletz River marine basalts of the Coast Range to the west and the volcanic and intrusive rocks of the Western Cascades to the east.

More near-surface material of low resistivity is evident between the Western and High Cascades in Figure 3 and may represent sediments and volcanics accumulated in the Cascades graben. Beneath the easternmost four stations of our profile in the Deschutes Basin, outcropping basaltic rocks give rise to values of ρ_{yx} around 100 ohm m at the shortest periods. They fall rapidly to about 20 ohm m as period increases to 1 s, however, with corresponding high values of ϕ_{yx}. Based just on skin depth computed using ρ_{yx}, these data indicate a low-resistivity layer only several hundred meters down. Examining more closely the Coast Range data, one sees ρ_{yx} falling from the shortest periods to a subtle minimum around 1 s, along with phases usually exceeding 45° over the same period range. Based again on skin depth arguments using ρ_{yx}, these data indicate the existence of an electrically conductive unit or layer over a depth range roughly of 1-2 km beneath the Siletz River volcanics. Structure off-line from the profile cannot be responsible since a minimum at around 1 s is seen in both ρ_{yx} and ρ_{xy}.. Beneath all the conductive structures described above lies a resistive basement and middle crust causing ρ_{yx} to rise and ϕ_{yx} to fall to 30° or less over the period range of 1-10 s.

The feature of the observations which has intrigued us the most is the ridge in ϕ_{yx} just below 100 s period extending across most of the Lincoln Line profile (Figure 3). The amplitude of the ridge is nearly 15° at the coast but decreases to only several degrees below the Coast Range and westernmost Willamette Valley (see Figure 4). However, the phase anomaly increases abruptly to the east starting beneath the central Willamette Valley and reaches values under the Western Cascades that exceed by 25° those at periods a decade

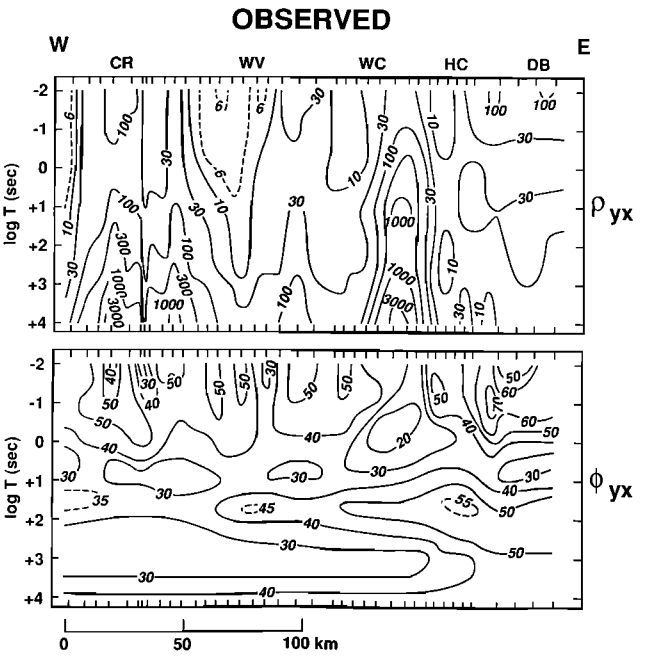

Fig. 3. Pseudosections of transverse magnetic apparent resistivity ρ_{yx} and impedance phase ϕ_{yx} observed along the landward portion of the Lincoln Line. Important physiographic and structural regions crossed include the Coast Range (CR), Willamette Basin (WB), Western Cascades (WC), High Cascade (HC), and Deschutes Basin (DB). Zero tick on scale bar corresponds to coastline. Numerical values for contouring are from field data of 39 broadband and 15 long-period MT sites smoothed and merged by P. Wannamaker. Color versions of these pseudosections appear in Plate 1 in the separate color section of this issue.

above and below. The subtle inflection in ρ_{yx} below the Coast Range which corresponds to the small phase peak described is not discerned easily in the apparent resistivity pseudosection. When ρ_{yx} is plotted in sounding form, however, the inflection is clearly above the noise (Figure 4). East of the central Willamette Valley, an actual minimum in ρ_{yx} at around 100 s can be seen both in the apparent resistivity pseudosection and the sounding curves (e.g., Figure 5). The anomaly in ρ_{yx} and ϕ_{yx} strongly suggests the presence of a conductive layer whose conductivity-thickness product (conductance) increases markedly from west to east. Given the range of periods and apparent resistivities characterizing the anomaly, skin depth calculations suggest a depth of a few tens of kilometers for the layer. Note also that the layer appears to end or change abruptly near the High Cascades. Similar evidence for the layer, including its eastward increase in conductance, is visible in the mini-EMSLAB results to the south [*Young et al.*, 1988]. The amplitude of our anomaly is considerably weaker, especially in the Coast Range, and occurs at somewhat longer periods, than that observed by *Kurtz et al.* [1986] on Vancouver Island. This probably results from much higher resistivities above and below the conductive layer beneath Vancouver Island, relative to those beneath the Coast Range, as implied by the generally high values of apparent resistivity of *Kurtz et al.* At present we consider the phase anomaly of Figure 3 to

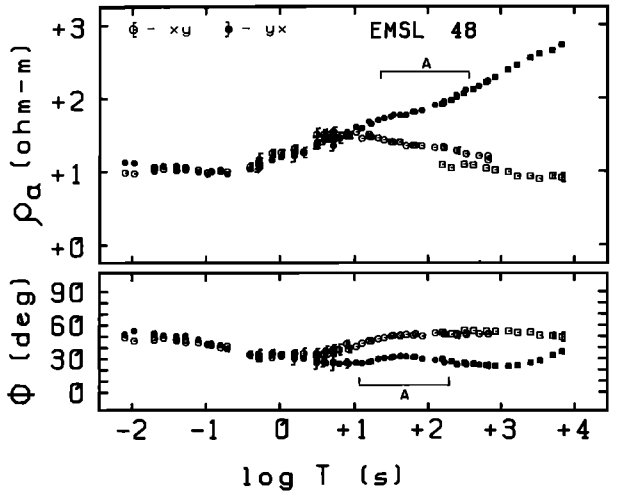

Fig. 4. Broadband (circles) and long-period (squares) MT data collected by the University of Utah Research Institute (UURI) and the Geological Survey of Canada (GSC) some 48 km inland on Lincoln Line. Displacement of about 1 km between broadband and long-period sites is responsible for small static offset in ρ_{xy}. The long-period anomaly in ϕ_{yx} presumed to be associated with subduction (A) is at its weakest in this area. Error bars are one standard deviation where they exceed the size of the plotting symbols.

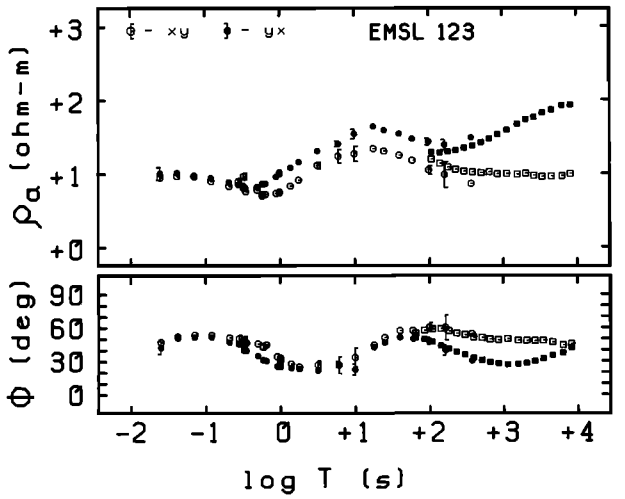

Fig. 5. Broadband and long-period MT data collected by the University of Oregon (circles) and GSC (squares) about 123 km inland on the Lincoln Line.

be the most obvious manifestation of resistivity structure which may be associated with the subducting Juan de Fuca plate below Oregon. Especially close attention will be given to this anomaly in the interpretation papers in this issue, to define the permissible range of causative structure and its significance for physical conditions in the subduction zone.

A very substantial volume of resistive earth material lies below the conductive layer just described, presumably in the upper mantle. That is evident from the steep upturn in ρ_{yx}, plus the drop in ϕ_{yx} to less than 30°, at periods of about 100 s and longer (Figures 3-5). As was the case for the conductive layer, the deep high-resistivity material extends toward and may terminate under the High Cascades. The steep upturn in ϕ_{yx} at the very longest periods, 5000 s and beyond, plus the incipient rollover in ρ_{yx} here, show that the resistor possesses a lower limit beyond which resistivity decreases again. This final medium to which our data is sensitive, if the data can be shown not to be responding to some off-line (three-dimensional) structure, should lie at depths of hundreds of kilometers.

The results at longer periods east of the High Cascades, in the Deschutes Basin, are very different from those detailed above. We have no long-period MT impedance recordings east of Mount Jefferson but broadband data to 800 s have been obtained (Figure 6). At periods beyond about 30 s, a decrease in ρ_{yx} is quite apparent while ϕ_{yx} rises well above 50°. Our measurements here in the east, however, show no indication of the deep, high-resistivity material so obvious west of the High Cascades. Interpretation of these data may be complicated by their proximity to a major east trending boundary in resistivity between the Blue Mountains block to the north and the Basin and Range to the south [*Gough et al.*, this issue], so that the assumption of a two-dimensional model in this region should be treated with caution. The geomagnetic array coverage may be especially useful here in constraining our model structures. Nevertheless, it is obvious that a fundamental electrical boundary exists almost directly under the High Cascades.

In Figure 7 and Plate 2 are the pseudosections of apparent resistivity and impedance phase of the transverse magnetic mode of the sea floor data. (Plate 2 can be found in the separate color section of this issue.) In contrast to the land apparent resistivity, we see only a smooth variation from west to east in the offshore results, suggesting minimal effects by shallow lateral inhomogeneity local to the individual measurement sites. The western two soundings at the shortest periods exhibit high values of impedance phase and apparent resistivities which fall rapidly with period from values around 100 ohm m. Based on skin depth using apparent resistivity, these results indicate a pronounced

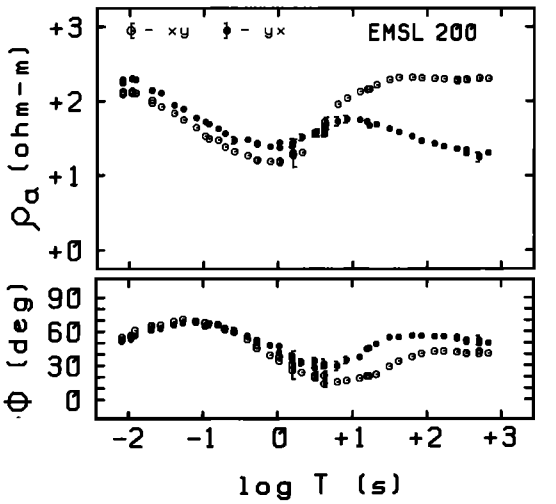

Fig. 6. Broadband MT sounding collected by UURI about 200 km inland on the Lincoln Line (its easternmost site of Figure 2). Observe the lack of evidence for the deep conductive layer which was apparent in ρ_{yx} and ϕ_{yx} west of the High Cascades.

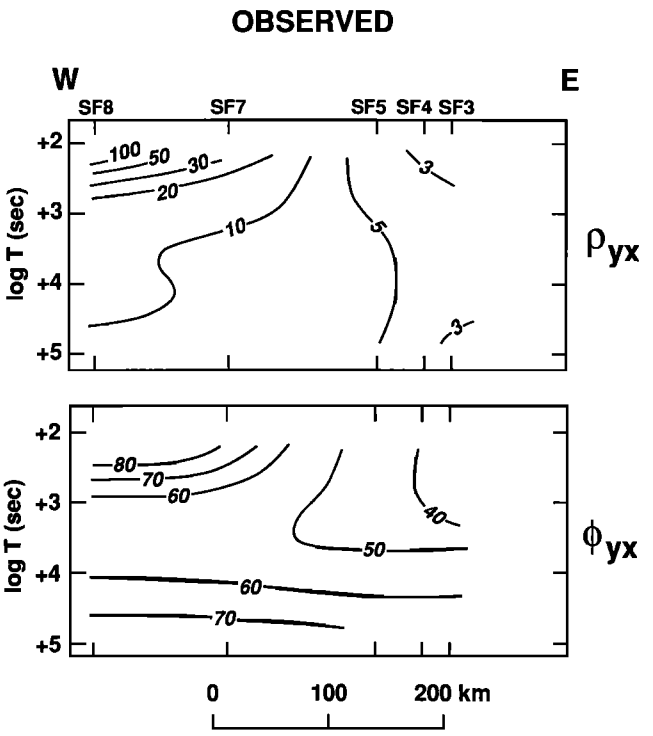

Fig. 7. Pseudosections of transverse magnetic apparent resistivity ρ_{yx} and impedance phase ϕ_{yx} observed at the five MT soundings on the ocean bottom segment of the Lincoln Line. All electric field recording instruments and four of the magnetic recorders were designed and built by J. Filloux. The magnetic variometer at SF8 was constructed by T. Yukutake, J. S. Segawa and colleagues, that at SF1 was produced by L. Law, and that at SF2 by A. White. Color versions of these pseudosections appear in Plate 2 in the separate color section of this issue.

transition from low resistivity in the upper few tens of kilometers to high resistivity below. The high resistivity region may represent the asthenosphere of the Juan de Fuca plate. In the TE data at SF7, a minimum in ϕ_{xy} and an inflection in ρ_{xy} around 2000 s period at first glance suggest that somewhat more resistive mantle material lies beneath the aforesaid conductive zone. This subtle characteristic however is not shared by the site closest to the ridge, SF8, nor by the westernmost sites SG4 and SE3 off the Lincoln Line and thus cannot be considered typical of the sea floor soundings.

Toward the east end of the ocean bottom profile, the soundings appear increasingly affected by conductive material at relatively shallow depths. The apparent resistivities at the shortest periods, say 200 s, progress from about 10 ohm m at SF5 to 3 ohm m at SF3. The values of ϕ_{yx} less than 45° and the upturn in ρ_{yx} at periods below 1000 s at these three sites is indicative of underlying resistive material. The high-level but large-scale conductor manifest here probably is the thick wedge of deposited and accreted sediments associated with the subducted slab. The response of this wedge conductor appears to be screening evidence for any possible low-resistivity asthenosphere as suggested at the western sites. In the TM mode, the E-W limits of the sedimentary conductor act to keep ρ_{yx} low at the eastern sea floor sites from the shortest through the longest periods measured. Contributing to this effect also may be the thinning and termination of the seawater toward the coast [*Ranganayaki and Madden*, 1980]. A graphic consequence of the wedge and seawater edge structures is the more vertical orientation of the apparent resistivity contours as we approach the eastern end of the profile. Finally, all five soundings at the very longest periods, greater than 10^4 s, show ϕ_{yx} increasing again to values over 60° with ρ_{yx} decreasing. This behavior occurs more obviously in the TE mode (e.g., Figure 8). On the face of it, the deepest structure we have sensed on the sea floor, with a scale of hundreds of kilometers, has resistivity which is very low. The relationship between this conductor and the deepest unit, also conductive, inferred from the land data is not clear at present.

Transverse Electric Impedance Functions

Over purely two-dimensional structures, the TE mode response functions ρ_{xy} and ϕ_{xy} behave much more simply than do the TM functions. This is because the electric field E_x is parallel to resistivity contacts everywhere so that boundary charge effects do not arise. Consequently, the influence upon both ρ_{xy} and ϕ_{xy} of relatively large, deep structures may emerge toward longer periods without static distortion by small-scale resistivity variations near the surface. The two-dimensional TE mode response in that sense resembles the response of one-dimensional or layered earths. Based on this characteristic, the TE mode impedance data, identified from field data by its correlation with H_z, often is used to construct one-dimensional resistivity models

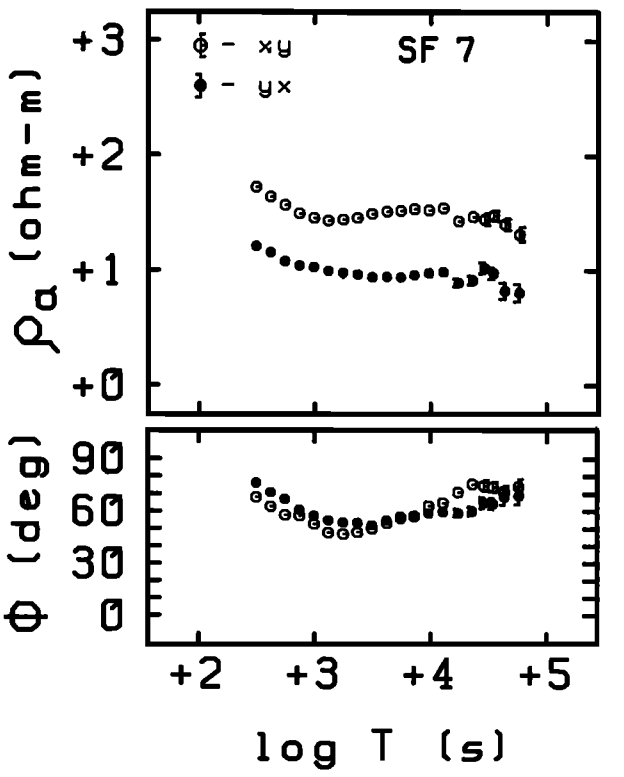

Fig. 8. Apparent resistivity and impedance phase responses at ocean bottom site SF7. Error bars are one standard deviation where they exceed the size of the plotting symbols.

at individual MT sites when two-dimensional effects seem apparent in the measurements [*Word et al.*, 1971]. Unfortunately, the TE results are very susceptible to deviations of the structure along strike (three-dimensional effects), which are apparent at least in the surficial geology beneath our transect and are likely to exist in the deep structures we are studying. Boundary charges do arise at such deviations and lead to static effects in ρ_{xy} that cannot be accommodated in purely two-dimensional TE modeling approaches [*Wannamaker et al.*, 1984]. Once again, the impedance phase is worth checking for evidence of any deep target, even though its contribution to the response may not be modeled correctly in terms of a two-dimensional structure.

Pseudosections of ρ_{xy} and ϕ_{xy} observed along the land segment of the Lincoln Line appear in Figure 9 and Plate 3. (Plate 3 can be found in the separate color section of this issue.) The pronounced vertical orientation of the apparent resistivity contours is as obvious here as it was in the TM mode data. Whereas the lateral variation in ρ_{xy} at short periods reflects differences in near-surface resistivity along the profile, its preservation to the longest periods means that these near-surface structures probably also vary substantially perpendicular to the profile as discussed just above. The signatures of the Willamette Basin and Cascades graben conductors perhaps provide the clearest examples of such end effects. Values of ϕ_{xy} of 30° or less around 10 s period plus a corresponding upturn in ρ_{xy} signify the resistive basement and middle crust. The rather shallow conductive layers beneath the Coast Range and the High Cascades and Deschutes Basin volcanics, inferred from the TM mode data at short periods, are evident in the pseudosections of ρ_{xy} and ϕ_{xy} also.

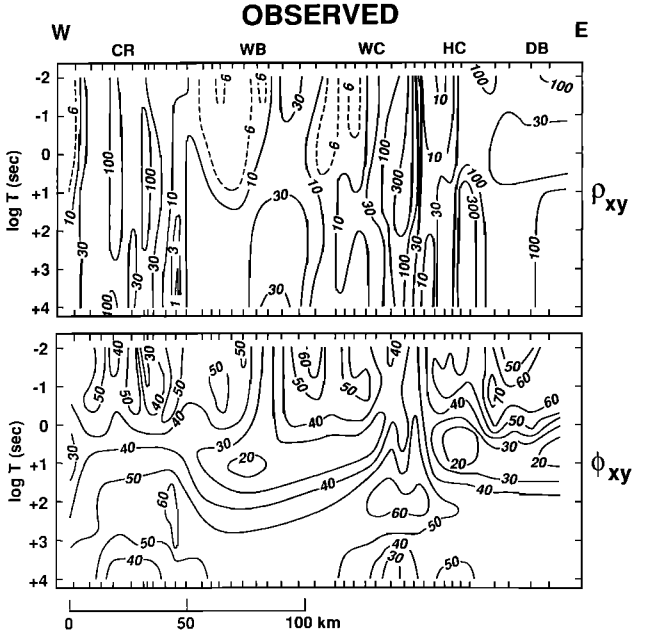

Fig. 9. Pseudosections of transverse electric apparent resistivity ρ_{xy} and impedance phase ϕ_{xy} observed along the landward portion of the Lincoln Line. Construction and labeling otherwise are similar to TM data of Figure 3. Color versions of these pseudosections appear in Plate 3 in the separate color section of this issue.

Noteworthy is the lack of an obvious expression of the subduction system in the TE mode results of Figure 9. In contrast to the TM mode, no sharp peak in ϕ_{xy} or inflection in ρ_{xy} is visible in the period range 30-100 s. There is instead an overall decrease in the TE apparent resistivity plus generally high values of phase (~50°) at periods of 100 s and longer. One possible factor contributing to the TE behavior may be variations in the inferred deep conductive layering along strike. In fact, there is a major westward shift in the Cenozoic volcanic front [*EMSLAB Group*, 1988] only 50 km north. The mini-EMSLAB results 50 km to the south described by *Young et al.* [1988] support this conjecture. At site 5 of that study, one observes an actual peak in ϕ_{xy} and an inflection in ρ_{xy} around 100 s period suggesting that the deep conductive unit is responding in a somewhat more one-dimensional manner farther away from the possible discontinuity. The TE mode data of *Kurtz et al.* [1986] appear to show the conductive layer below Vancouver Island more clearly, perhaps again due to higher resistivities above and below that layer.

There are other puzzling complexities observed in ρ_{xy} and ϕ_{xy} at long periods on land. The high values of phase and steeply declining apparent resistivities around 100 s beneath the Western Cascades may primarily represent the decaying influence of high resistivities in the upper and middle crust of this area. However, the narrow anomaly of high ϕ_{xy} and rapidly dropping ρ_{xy} at these periods about 40 km inland from the coast, plus those of increasing ρ_{xy} and low ϕ_{xy} at very long periods (2000-5000 s) around 25 and 135 km inland are especially problematic because their lateral extent seems so limited relative to the penetration depth of the incident fields. One may only speculate on the existence of some three-dimensional electrical connection or coupling between narrow, shallow structures and much larger ones below or off-line. We do not observe such problems in the TM mode data. *Wannamaker et al.* [this issue] present more quantitative demonstrations of the ability to fit the observations of ρ_{xy} and ϕ_{xy} with a purely two-dimensional model structure.

The TE mode response on the sea floor appears to be much simpler than that on land (Figure 10 and Plate 4). (Plate 4 can be found in the separate color section of this issue.) Off-profile problems are much less likely because of the fairly homogeneous near-surface sediment resistivity. Like the TM mode, the TE results show high resistivities in the lithosphere near the ridge with a substantial conductor below, as well as very low resistivities toward the east end of the line as it passes onto increasing sedimentary thicknesses. Perhaps the greatest difference in the two modes is apparent at moderate to short periods (less than about 3000 s) at the eastern three sites. Rather than remaining low from short through long periods, the TE apparent resistivity climbs very steeply as T increases from the shortest periods and is accompanied by very low values of impedance phase around 1000 s (Figure 11). Over moderate periods, 3000-10,000 s, ρ_{xy} reaches values of 30-40 ohm meters across the entire sea floor profile. We may be observing nearly two-dimensional behavior by ρ_{xy} and ϕ_{xy} at least in the upper two-thirds of the period range. The absence of problems that beset the land data, namely severe static distortions and other complex

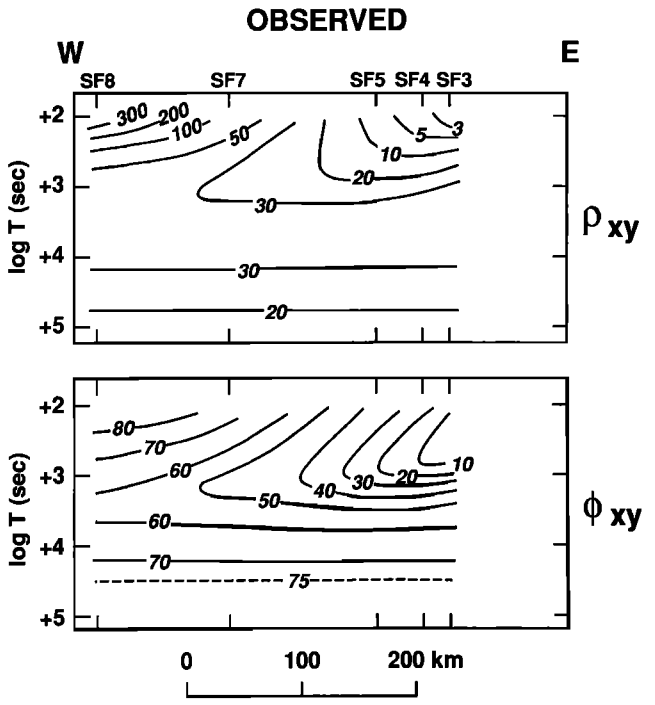

Fig. 10. Pseudosections of transverse electric apparent resistivity ρ_{xy} and impedance phase ϕ_{xy} observed along the sea floor segment of the Lincoln Line. Color versions of these pseudosections appear in Plate 4 in the separate color section of this issue.

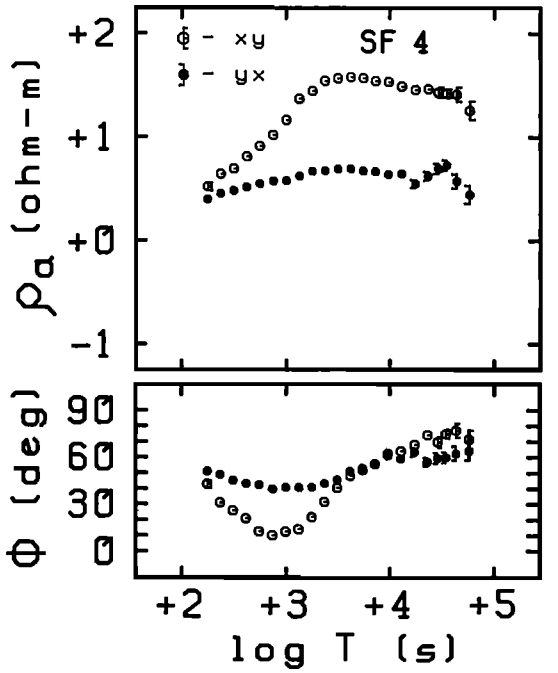

Fig. 11. Apparent resistivity and impedance phase responses for both TE and TM modes at ocean bottom site SF4.

three-dimensional effects, gives us hope that a model resistivity section is achievable for the ocean results that is largely in agreement with both modes of the MT impedance. For periods beyond 10^4 s, ρ_{xy} falls markedly and ϕ_{xy} exceeds 70° over the entire ocean line. The inference of an ultra-deep conductive region appears somewhat stronger here in the TE mode than in the TM, as mentioned earlier with Figures 7 and 8.

Vertical Magnetic Field Functions

As implied by equation (2), a vertical magnetic field exists only when there are lateral variations of resistivity in the Earth. Electric current flow concentrates in good conductors relative to poor ones, resulting in a circulation of the anomalous magnetic field about the structures in accordance with Ampère's law. For example, element M_{zy} across an isolated two-dimensional conductive axis exhibits a reversal of sign. If resistivity merely increases in one direction (-y or +y) across strike, a simple peak (positive or negative) results. Individual resistivity structures, including three-dimensional ones, tend to respond over a limited period range in a fashion similar to the impedance phase [*Wannamaker et al.*, 1984]. Thus the vertical magnetic field also favors recognition of deep structures beneath complex near-surface heterogeneity. Furthermore, M_{zy} is affected less adversely than the TE mode impedance by interruptions of a structural trend along strike. Specifically, the basic geometry of the anomalies (e.g., location and shape of peaks or crossovers) tends to remain although their amplitudes and breadths of period range can differ.

The vertical magnetic field response along the landward portion of the Lincoln Line (Figure 12 and Plate 5) appears to support and augment inferences drawn previously from the transverse magnetic impedance functions. (Plate 5 can be found in the separate color section of this issue). In the vicinity of the coastline, a strong positive anomaly in the real component of M_{zy}, denoted $Re(M_{zy})$, shows an

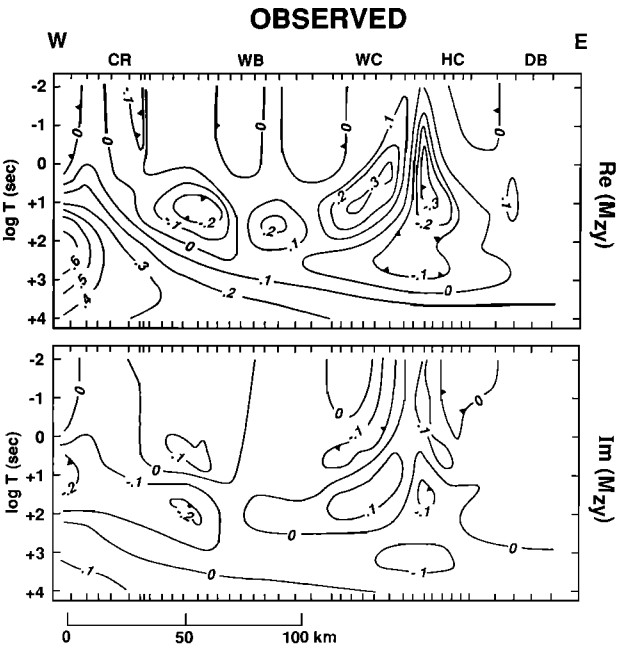

Fig. 12. Pseudosections of vertical magnetic field transfer function M_{zy}, real and imaginary components, observed along the land segment of the Lincoln Line. Contour values are dimensionless. Color versions of these pseudosections appear in Plate 5 of the separate color section of this issue.

amplitude maximum around 300 s period, below which it weakens but spreads laterally. By 10,000 s, values exceeding 0.1 underlie the entire line. The associated imaginary component $Im(M_{zy})$ is more subdued in its range than the real, showing negative amplitudes around 10-100 s near the coast but becoming positive at longer periods. The most obvious candidate to explain the aforesaid vertical field response is the conductive seawater of the Pacific Ocean. That hypothesis may be verified using a two-dimensional computer algorithm, however, since the bathymetry is oriented predominantly N-S and the resistivity of the seawater is well constrained [*Filloux,* 1987]. Whatever portion of the response cannot be explained by the known seawater provides information on the volume of conductive sediments offshore, in the trench melange for instance, and also perhaps about the deep asthenosphere below the Juan de Fuca plate.

Sediments of the Willamette Basin affect the response of M_{zy} in Figure 12 over about the central half of the Lincoln Line and the period range 1-100 s. The negative peak in $Re(M_{zy})$ associated with this confined conductor lies about 50 km inland with the values becoming positive east of about y = 75 km. While this sign reversal probably signifies the point of greatest sediment thickness, the presence of two positive peaks at y = 85 km and from 120-135 km indicates either another depth maximum around 100 km inland or perhaps an increase in basement resistivity farther east. The values near zero of both real and imaginary M_{zy} over the central Willamette Basin at periods shorter than about 1 s reflect less the absence of a structural response at shallow levels than they do the erratic and unreliable character of the data here due to strong cultural interference. The loss of these results prevents confirmation of the thickness of the Columbia River basalt flows in this area as inferred from the impedance functions.

Examples of the observations taken at individual MT sites near the western and eastern margins of the Willamette Basin are plotted in Figures 13 and 14. We observe first the excellent agreement between the broadband and long-period data in their common period range of 60-300 s at both stations. In Figure 13, the amplitude of M_{zy}, both real and

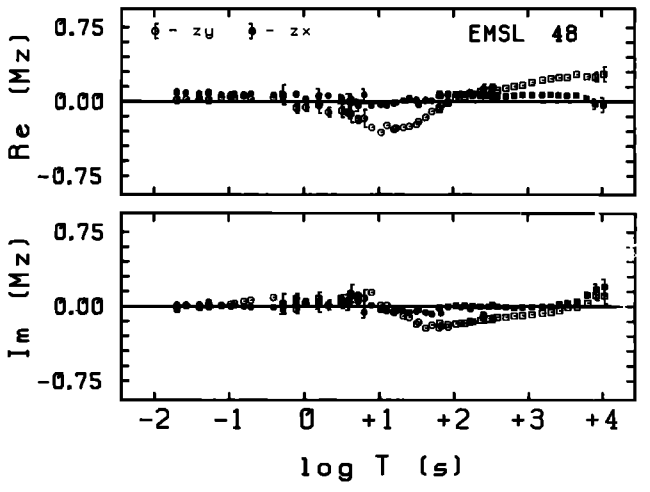

Fig. 13. Real and imaginary response curves for elements M_{zx} and M_{zy} measured by UURI and GSC about 48 km inland. Error bars are one standard deviation where they exceed the size of the plotting symbols.

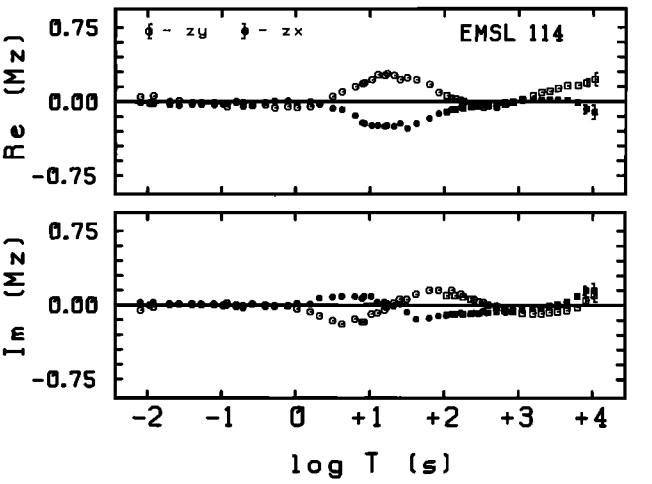

Fig. 14. Real and imaginary response curves for elements M_{zx} and M_{zy} measured by UURI and GSC about 114 km inland.

imaginary components, greatly exceeds that of M_{zx} over almost the entire period range, thereby substantiating our assumption of N-S trending geoelectric structures at least in this area. Obvious in the raw data here is the negative in $Re(M_{zy})$ around 10-20 s signifying the Willamette Basin. Also, the positive in this quantity developing beyond 100 s is evidence for the Pacific Ocean and other large-scale heterogeneity. On its eastern side, the effect of the basin on M_{zx} is nearly as great as on M_{zy} (Figure 14) and the coordinate rotation which minimizes M_{zx} yields a geoelectric strike of about N35°E. The predominance of M_{zy} returns below 100 *s,* however, showing that deeper structures are still aligned nearly N-S. Following a subtle excursion to below zero from 100-1000 s, $Re(M_{zy})$ at the longest periods displays the positive values ubiquitous to the Lincoln Line.

There is a strong negative response in $Re(M_{zy})$ associated with the western boundary of the Cascades graben located about 145 km inland (Figure 12). The lack of a positive counterpart to the east indicates that the conductive fill of the graben does not terminate as abruptly on this side but instead merges, or nearly does, with the shallow conductive layer of the Deschutes Basin region as implied from the impedance functions of Figure 3, 6, and 7. This response of the graben structure attenuates rapidly as periods reach 100 s. At somewhat longer periods however, 100-1000 s specifically, an additional negative anomaly in $Re(M_{zy})$ is resolved in this area (Figure 15) [see *EMSLAB Group,* 1988]. The anomaly is strongest between the Western and High Cascades but negative values extend west to within 100 km of the coast (as was seen in Figure 14). Given the persistence westward, the response cannot be due solely to the abrupt transition in deep conductivity from west to east below the High Cascades, most obvious in Figure 3, although that transition probably contributes. We believe this negative in $Re(M_{zy})$ thus is providing independent corroboration of the deep layer of high conductance extending from the central Willamette Basin to the High Cascades brought to light by the TM mode observations. The peak negative response near y = 145 km may in part also be due to a conductive axis associated with the present volcanic arc, a hypothesis to be tested in subsequent papers on interpretation.

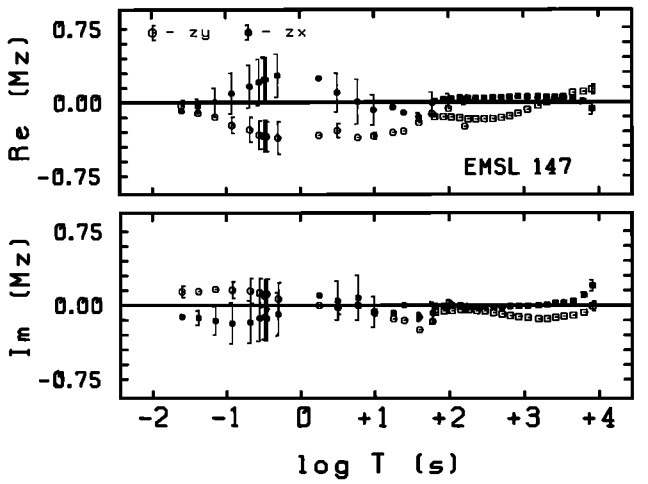

Fig. 15. Real and imaginary response curves for elements M_{zx} and M_{zy} measured by University of Oregon and GSC about 147 km inland on the Lincoln Line.

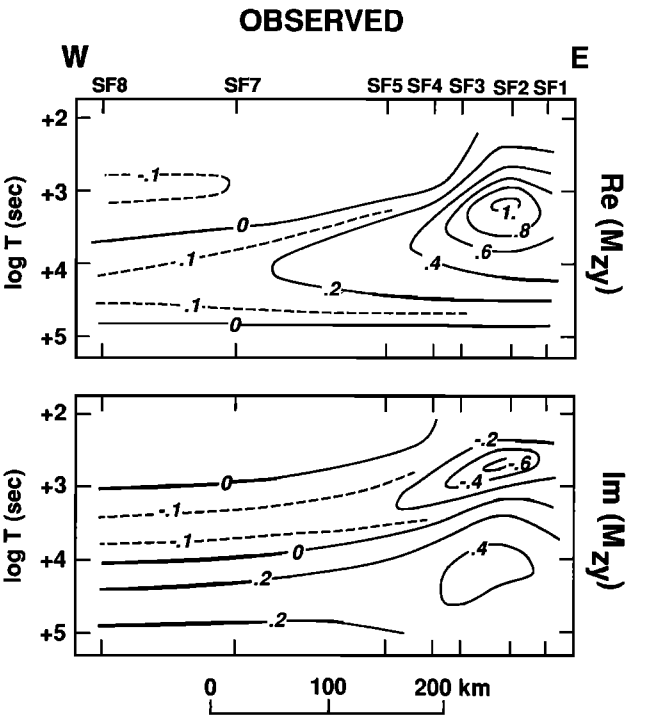

Fig. 16. Pseudosections of vertical magnetic field transfer function M_{zy}, real and imaginary components, observed along the sea floor portion of the Lincoln Line. Contour values are dimensionless. Color versions of these pseudosections appear in Plate 6 of the separate color section of this issue.

On the ocean bottom, we have seven geomagnetic variation soundings to characterize the vertical field response over the Juan de Fuca plate along the Lincoln Line. By far the most striking feature of the observations (Figure 16 and Plate 6) is the enormous positive anomaly in $Re(M_{zy})$ at the eastern four sites some 50-100 km offshore, reaching unity at SF2, with complementary behavior by the imaginary component. (Plate 6 can be found in the separate color section of this issue.) Anomalies in M_{zy} on the sea floor, we should point out, may be amplified by the overlying seawater at peak periods because current flow induced in the water substantially reduces the horizontal H field below it. The aforesaid anomaly occurs near the ocean floor-continental shelf break where water depth starts diminishing most rapidly to the east. The vertical magnetic field nevertheless should also carry information about structure beneath the ocean floor, for instance, the conductive sediment melange. By constraining the effect of the seawater in the same manner as for the land data, the existence of such structure may be ascertained through two-dimensional simulations. However, there is no discernible response in M_{zy} that may be associated with a conductive axis beneath the spreading ridge. This is supported by other EMSLAB geomagnetic stations near the ridge crest not on the Lincoln Line and also by earlier observations and modeling of *Law and Greenhouse* [1981] across the ridge north of the EMSLAB array.

The major anomaly in M_{zy} just described decreases rapidly as period falls below 10,000 s and appears to reach zero around 10^5 s (Figure 16) The rate at which M_{zy} responses decay at long periods is a function of the resistivity below the causative structure [*Wannamaker et al.*, 1984]. The relatively steep decrease visible in the pseudosection suggests that conductive material of regional extent exists well down into the mantle. Candidates for the material include the conductive asthenosphere inferred previously from both the TM and TE impedance functions and perhaps also the very deep conductor evident at periods beyond 10^4 s. Finally, a very large scale three-dimensional inhomogeneity is indicated at periods greater than 10^4 s by element M_{zx}, which we include in the plot of the response functions at site SF5 (Figure 17). For

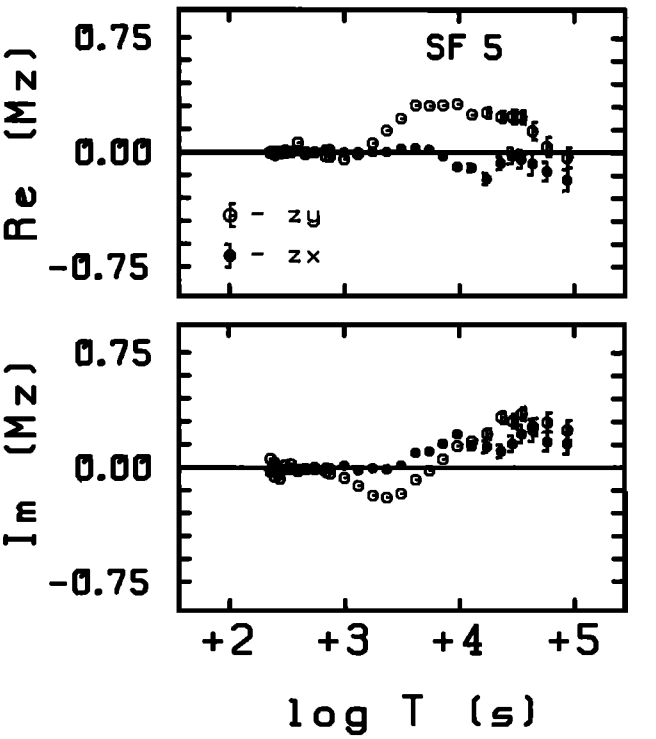

Fig. 17. Real and imaginary response curves for M_{zx} and M_{zy} at ocean bottom site SF5. Error bars are one standard deviation where they exceed the size of the plotting symbols.

the x-y-z coordinate system adopted in EMSLAB, which is that specified with equations (1) and (2), the negative values of $Re(M_{zx})$ and positive values of $Im(M_{zx})$ observed at periods beyond 10^4 s in Figure 17 and over the whole sea floor line imply that a lateral transition to higher deep resistivity should exist south of the sea floor array. Such behavior in $Re(M_{zx})$ appears at the longest periods of the land data as well (Figures 13-15).

CONCLUSIONS

We have collected a magnetotelluric data set of high quality that is richly informative about the resistivity expression of the Juan de Fuca subduction system. Upper crustal conductive units apparent upon inspection of the land observations include massive sedimentary fill of the Willamette Basin as well as layers beneath the Coast Range, from the Western to the High Cascades, and in the Deschutes Basin area. All are underlain by resistive basement and middle crust. Especially relevant to the subduction process beneath the continent we believe is a conductive, roughly horizontal layer at a depth of a few tens of kilometers in otherwise resistive lower crust and upper mantle which extends eastward from the coast and changes abruptly at the High Cascades. A fundamental transition in deep resistivity to that beneath the Deschutes Basin occurs below the active High Cascades volcanic arc. Seafloor MT soundings over the Juan de Fuca plate near the spreading ridge imply a highly conducting region at depths of some tens of kilometers that may represent the asthenosphere. Toward the coast, a conductive wedge of sediments increasingly influences the MT and geomagnetic soundings. Probably our best prospect for determining an accurate resistivity model from the observed data is to interpret the data carefully assuming a two-dimensional resistivity variation with a N-S strike. For such an analysis, the TM mode impedance functions should be emphasized since they are more robust to common deviations from the two-dimensional assumption, with the vertical magnetic field and the TE impedance examined also for consistency and additional information. It should be clear from our discussions, however, that certain important features of the data ultimately will be understood only in terms of fully three-dimensional geometries.

Valuable lessons have been learned about the collection of magnetotelluric data in complex natural environments. First, observations of high statistical accuracy are required to resolve certain key features of the resistivity structure. The anomaly in ρ_{yx} around 30-50 s period beneath the Coast Range, which is the most likely manifestation of subduction structure in this region, is only of several degrees amplitude. Luckily, the response occurred at periods where the natural fields are strong and cultural interference is relatively subdued. We cannot count on such good fortune always, and high quality data at shorter periods are important more generally for understanding upper crustal heterogeneity. It is therefore highly desireable for the future that the broadband MT instrumentation incorporate full remote reference capability (sensor separations of 10 km or more) and statistically robust processing to ensure sounding curves that are accurate over all periods. Second, the rate of collection of MT data by research institutions is painfully slow and exhausting due again to the state of the field systems. Highly desireable improvements in broadband instrumentation include acquisition of the mid- and low-band data simultaneously, complete in-field data processing to yield a finished sounding on-site, and the ability to deploy additional electric field bipoles (especially E_y) independent of the magnetic field apparatus. Similarly, improvements in sea floor instrumentation to take advantage of modern electronic developments would increase our ability to utilize MT in the oceans. While better data analysis has increased the usable period range on the sea floor, the shortest periods attainable at present are limited by magnetometer sensitivity. Implementation of the foregoing recommendations is essential we believe if the productivity of magnetotelluric profiling is to approach that of reflection seismic profiling.

Acknowledgments. We wish to acknowledge the following sources of funding support which made the project possible: U.S. National Science Foundation, grants EAR-8410638 and EAR-8512895; Natural Sciences and Engineering Research Council of Canada, Collaborative Special Grant A6892; Geological Survey of Canada; Ministry of Education, Science and Culture of Japan, Grant-in-Aid for Overseas Scientific Survey 61043014; Australian Research Grants Scheme, Flinders University and Australian Department of Science; Green's Foundation of the Scripps Institute of Oceanography; and AT & T Bell Laboratories. Second, we are very grateful to the U.S. Forest Service, Oregon State Department of Forestry, and the many private timber companies and land owners who permitted access to measurements on their properties. Finally, we are indebted to the numerous graduate students and technical assistants who worked on the field acquisition and reduction of our data. This is Geological Survey of Canada contribution 23388.

REFERENCES

Boehl, J. E., F. X. Bostick, Jr., and H. W. Smith, An application of the Hilbert transform to the magnetotelluric method, report, 98 pp., Electr. Geophys. Res. Lab., University of Tex. at Austin, 1977.

Bostick, F. X., Jr., Electromagnetic array profiling (EMAP), extended abstract of paper presented at the 56th annual meeting, Soc. of Explor. Geophys., Houston, Tex., 1986.

Chave, A. D., and D. J. Thomson, Some comments on magnetotelluric response function estimation, *J. Geophys. Res.*, this issue.

Chave, A. D., D. J. Thomson, and M. E. Ander, On the robust estimation of power spectra, coherences, and transfer functions, *J. Geophys. Res.*, *92*, 633–648, 1987.

Chave, A. D., J. H. Filloux, D. S. Luther, L. K. Law, and A. White, Observations of motional electromagnetic fields during EMSLAB, *J. Geophys. Res.*, this issue.

Clarke, J., T. D. Gamble, W. M. Goubou, R. H. Koch, and R. Miracky, Remote reference magnetotellurics: Equipment and measurement procedures, *Geophys. Prospect, 31*, 149–170, 1983.

Egbert, G. D., and J. R. Booker, Robust estimation of geomagnetic transfer functions, *Geophys. J. Roy. Astron. Soc., 87*, 173–194, 1986.

Egbert, G. D., and J. R. Booker, Multivariate analysis of geomagnetic array data, 1, The response space, *J. Geophys. Res.*, this issue.

EMSLAB Group, The EMSLAB electromagnetic sounding experiment, *Eos Trans. AGU, 69*, 89, 98–99, 1988.

Filloux, J. H., Instrumentation and experimental methods for oceanic studies, in *Geomagnetism, 1*, edited by J. A. Jacobs, Academic, San Diego, Calif., pp. 143–248, 1987.

Gamble, T. D., W. M. Goubau, and J. Clarke, Magnetotellurics with a remote reference, *Geophysics, 44*, 53–68, 1979*a*.

Gamble, T. D., W. M. Goubau, and J. Clarke, Error analysis for remote reference magnetotellurics: *Geophysics, 44*, 959–968, 1979*b*.

Gough, D. I., D. McA. McKirdy, D. V. Woods, and H. Geiger, Conductive structures and tectonics beneath the EMSLAB land array, *J. Geophys. Res.*, this issue.

Jiracek, G. R., J. H. Curtis, J. Ramirez, M. Martinez, and J. Romo, Two-dimensional magnetotelluric inversion modeling of the EMSLAB Lincoln Line, *J. Geophys. Res.*, this issue.

Jones, A. G., The problem of current channeling: a critical review, *Geophys. Surv., 6,* 79–122, 1983.

Jones, A. G., A. D. Chave, G. D. Egbert, D. R. Auld and K. Bahr, A comparison of techniques for magnetotelluric response function estimation, *J. Geophys. Res.*, this issue.

Kurtz, R. D., J. M. DeLaurier, and J. C. Gupta, A magnetotelluric sounding across Vancouver Island detects the subducting Juan de Fuca plate, *Nature, 321,* 596–599, 1986.

Law, L. K., and J. P. Greenhouse, Geomagnetic variation sounding of the asthenosphere beneath the Juan de Fuca Ridge, *J. Geophys. Res., 86,* 967–978, 1981.

Livelybrooks, D. W., W. W. Clingman, J. T. Rygh, S. A. Urquhart, and H. S. Waff, A magnetotelluric study of the High Cascades graben in central Oregon, *J. Geophys. Res.*, this issue.

Petiau, G., and A. Dupis, Noise, temperature coefficient, and long time stability of electrodes for telluric observations, *Geophys. Prospect, 28,* 792–804, 1980.

Price, A. T., The theory of geomagnetic induction, *Phys. Earth Planet. Inter., 7,* 227–233, 1973.

Ranganayaki, R. P., and T. R. Madden, Generalized thin sheet analysis in magnetotellurics: An extension of Price's analysis, *Geophys. J. Roy. Astron. Soc., 60,* 445–457, 1980.

Sims, W. E., F. X. Bostick, Jr., and H. W. Smith, The estimation of magnetotelluric impedance tensor elements from measured data, *Geophysics, 36,* 938–942, 1971.

Stodt, J. A., Noise analysis for conventional and remote reference magnetotellurics, Ph.D. thesis, University of Utah, Salt Lake City, 220 pp., 1983.

Vozoff, K. (Ed.), *Magnetotelluric Methods, Geophys. Reprint Series,* vol. 5, 800 pp., Soc. of Explor Geophys., Tulsa, Okla., 1986.

Waff, H. S., J. T. Rygh, D. W. Livelybrooks, and W. W. Clingman, Results of a magnetotelluric traverse across western Oregon: Crustal resistivity structure and the subduction of the Juan de Fuca plate, *Earth Planet. Sci. Lett., 87,* 313–324, 1988.

Wannamaker, P. E., G. W. Hohmann, and S. H. Ward, Magnetotelluric responses of three-dimensional bodies in layered earths, *Geophysics, 49,* 1517–1533, 1984.

Wannamaker, P. E., J. R. Booker, A. G. Jones, J. H. Filloux, A. D. Chave, H. S. Waff, and L. K. Law, Resistivity cross section through the Juan de Fuca subduction system and its tectonic implications, *J. Geophys. Res., this issue.*

Wight, D. E., and F. X. Bostick, Jr., Cascade decimation-a technique for real time estimation of power spectra, in *Proceedings IEEE International Conference on Acoustic Speech and Signal Processing,* pp. 626–629, IEEE, New York, 1980.

Word, D. R., H. W. Smith, and F. X. Bostick, Jr., Crustal investigations by the magnetotelluric impedance method, in *The Structure and Physical Properties of the Earth's crust, Geophys. Monogr. Ser.,* vol. 14, edited by J. G. Heacock, pp. 145–156, AGU Washington, D. C., 1971.

Young, C. T., and M. R. Kitchen, A magnetotelluric profile in the Coast Range of Oregon, *J. Geophys. Res.*, this issue.

Young, C. T., J. R. Booker, R. Fernandez, G. R. Jiracek, M. Martinez, J. C. Rogers, J. A. Stodt, H. S. Waff, and P. E. Wannamaker, Verification of five magnetotelluric systems in the mini-EMSLAB experiment, *Geophysics, 53,* 553–557, 1988.

J. R. Booker, Geophysics Program, AK-50, University of Washington, Seattle, WA 98195.

A. D. Chave, AT&T Bell Laboratories, Rm 1E-444, 600 Mountain Ave., Murray Hill, NJ, 07974.

G. D. Egbert, College of Oceanography, Oregon State University, Corvallis, OR, 97331.

J. H. Filloux, Scripps Institution of Oceanography, MS A-030, University of California at San Diego, La Jolla, CA 92093.

A. W. Green, Jr., U. S. Geological Survey, Denver Federal Center, P. O. Box 25046, Denver, CO 80225.

G. R. Jiracek, Department of Geological Sciences, San Diego State University, San Diego, CA 92182.

A. G. Jones, Lithospheric Geophysics, Geological Survey of Canada, 1 Observatory Crescent, Ottawa, Ontario, Canada, K1A 0Y3.

L. K. Law, Pacific Geoscience Center, Geological Survey of Canada, P. O. Box 6000, Sidney, British Columbia, Canada V8L 4BZ

M. Martinez G., Center for Scientific Research and Graduate Education of Ensenada (CICESE), Avenida Espinoza 843, 2732-Ensenada, Baja California, Mexico.

J. S. Segawa, Ocean Research Institute, University of Tokyo, 1-15-1 Minamidai Nakano, Tokyo 164, Japan.

J. A. Stodt, University of Utah Research Institute, 391-C Chipeta Way, Salt Lake City, UT 84108.

P. Tarits, Institute de Physique du Globe, Laboratoire de Geomagnetisme, 4 Place Jussieu, 75252 Paris Cedex 05, France.

H. S. Waff, Department of Geology, University of Oregon, Eugene, OR 97403.

P. E. Wannamaker, University of Utah Research Institute, 391-C Chipeta Way, Salt Lake City, UT 84108.

A. White, School of Earth Science, Flinders University of South Australia, Bedford Park, S. A. 5042, Australia

C. T. Young, Department of Geology and Geological Engineering, Michigan Technical University, Houghton, MI, 49931.

T. Yukutake, Earthquake Research Institute, University of Tokyo, Bunkyo-ku, Tokyo 113, Japan.

(Received May 13, 1988;
revised April 3, 1989;
accepted April 3, 1989.)

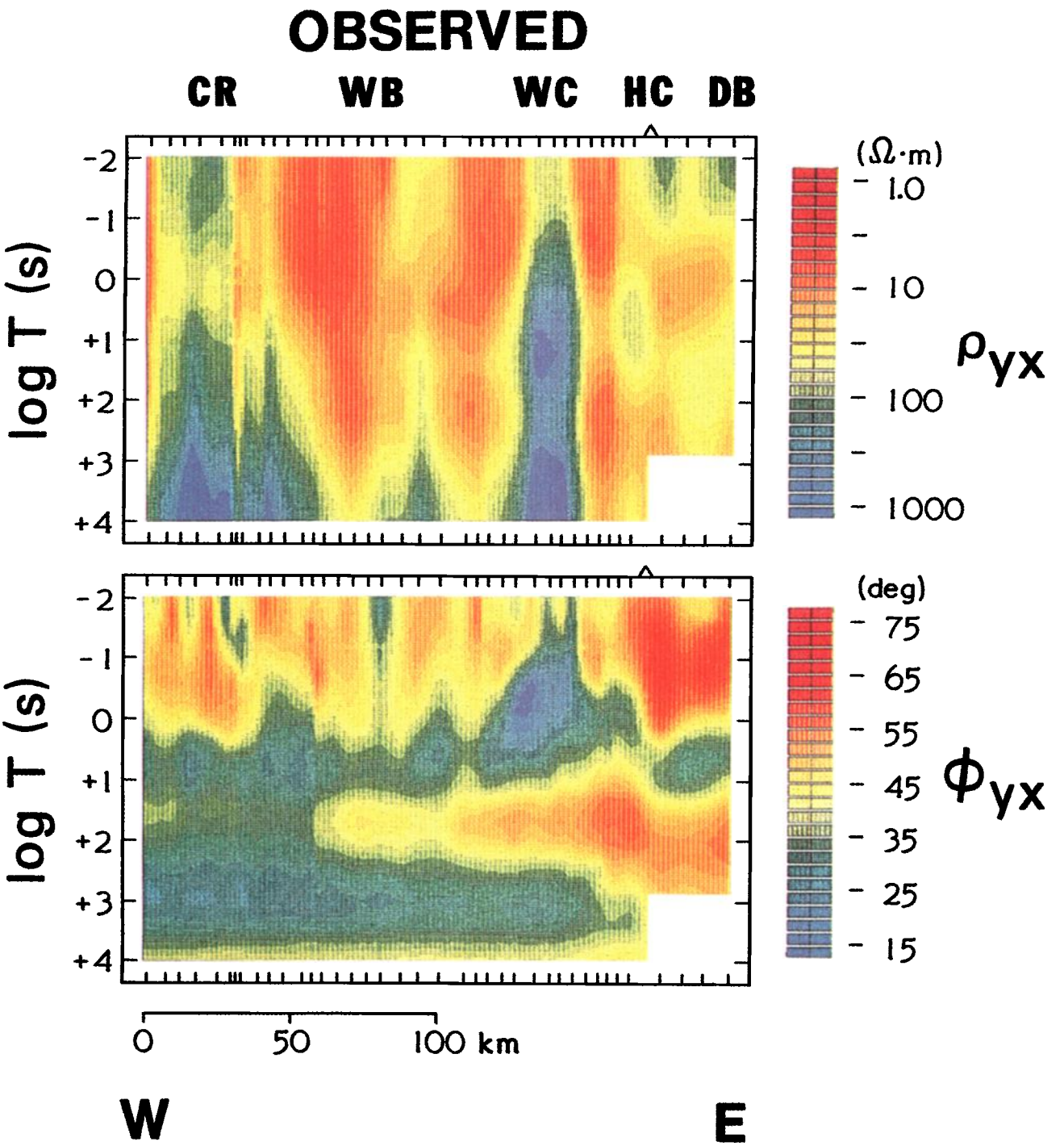

Plate 1. [*Wannamaker et al.*]. Pseudosections of transverse magnetic apparent resistivity ρ_{yx} and impedance phase ϕ_{yx} observed along the landward portion of the Lincoln Line.

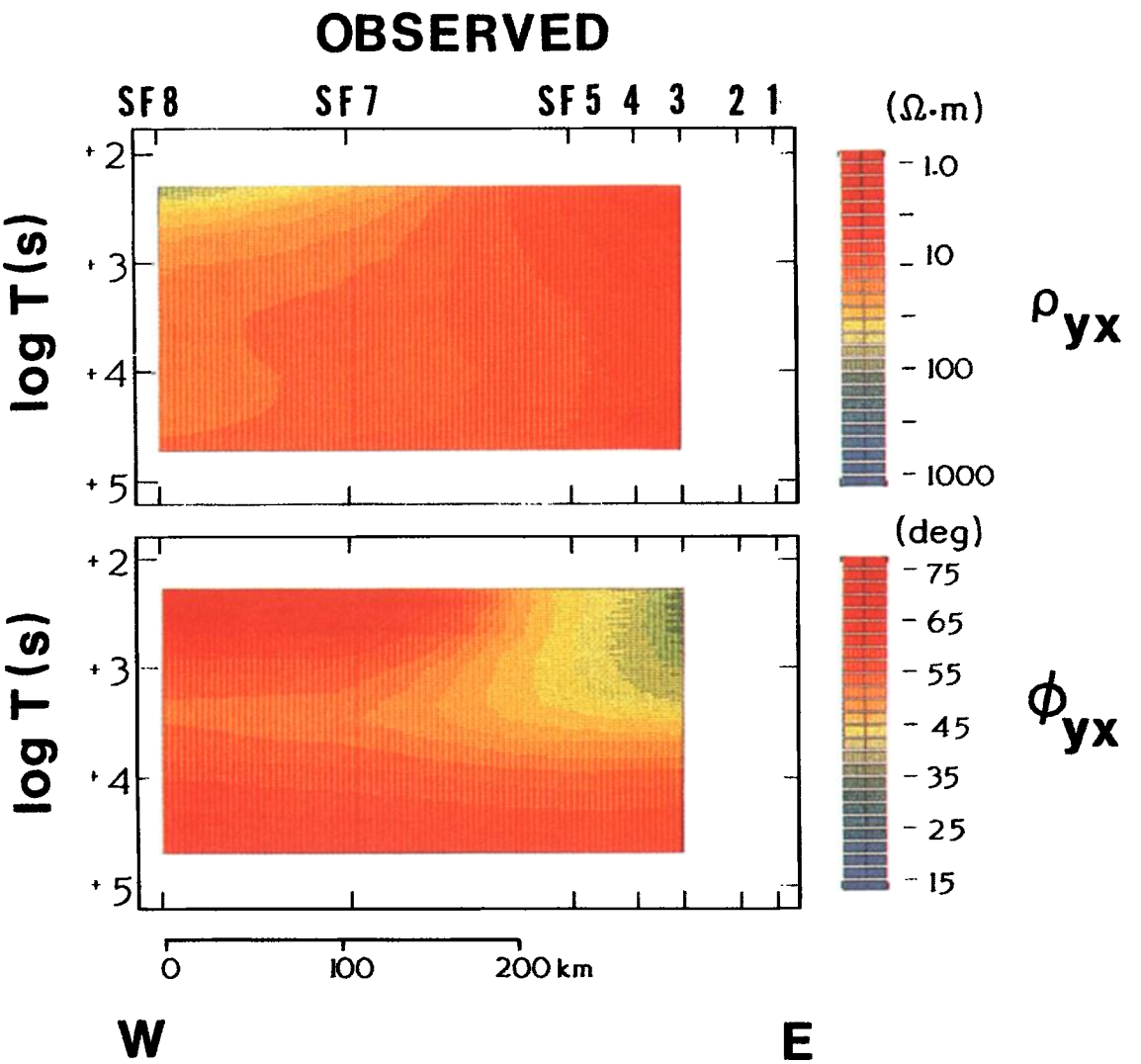

Plate 2. [*Wannamaker et al.*]. Pseudosections of transverse magnetic apparent resistivity ρ_{yx} and impedance phase ϕ_{yx} observed along the sea floor portion of the Lincoln Line. Note differences in horizontal scale and period range between land and sea floor results.

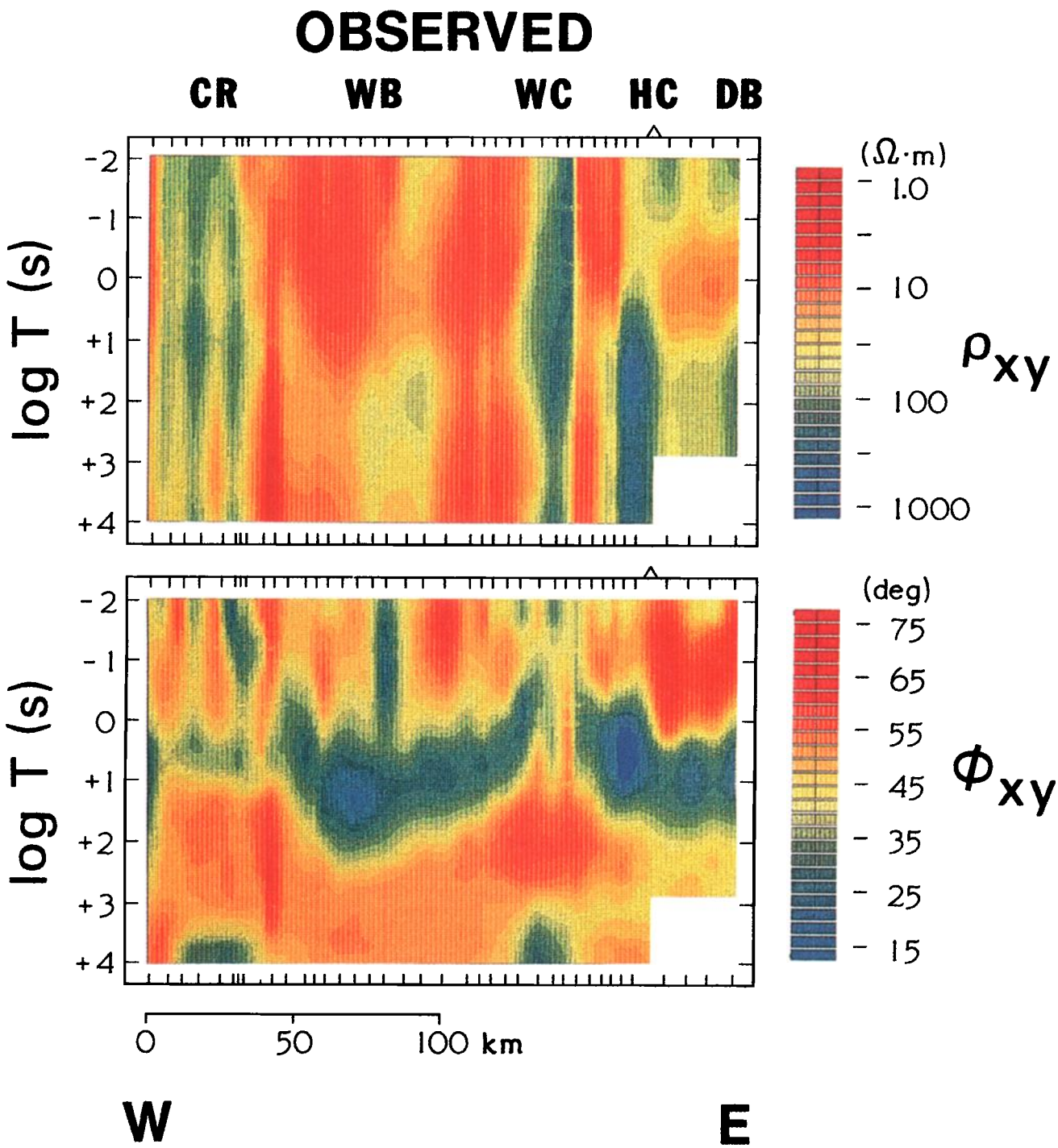

Plate 3. [*Wannamaker et al.*]. Pseudosections of transverse electric apparent resistivity ρ_{xy} and impedance phase ϕ_{xy} observed along the landward portion of the Lincoln Line.

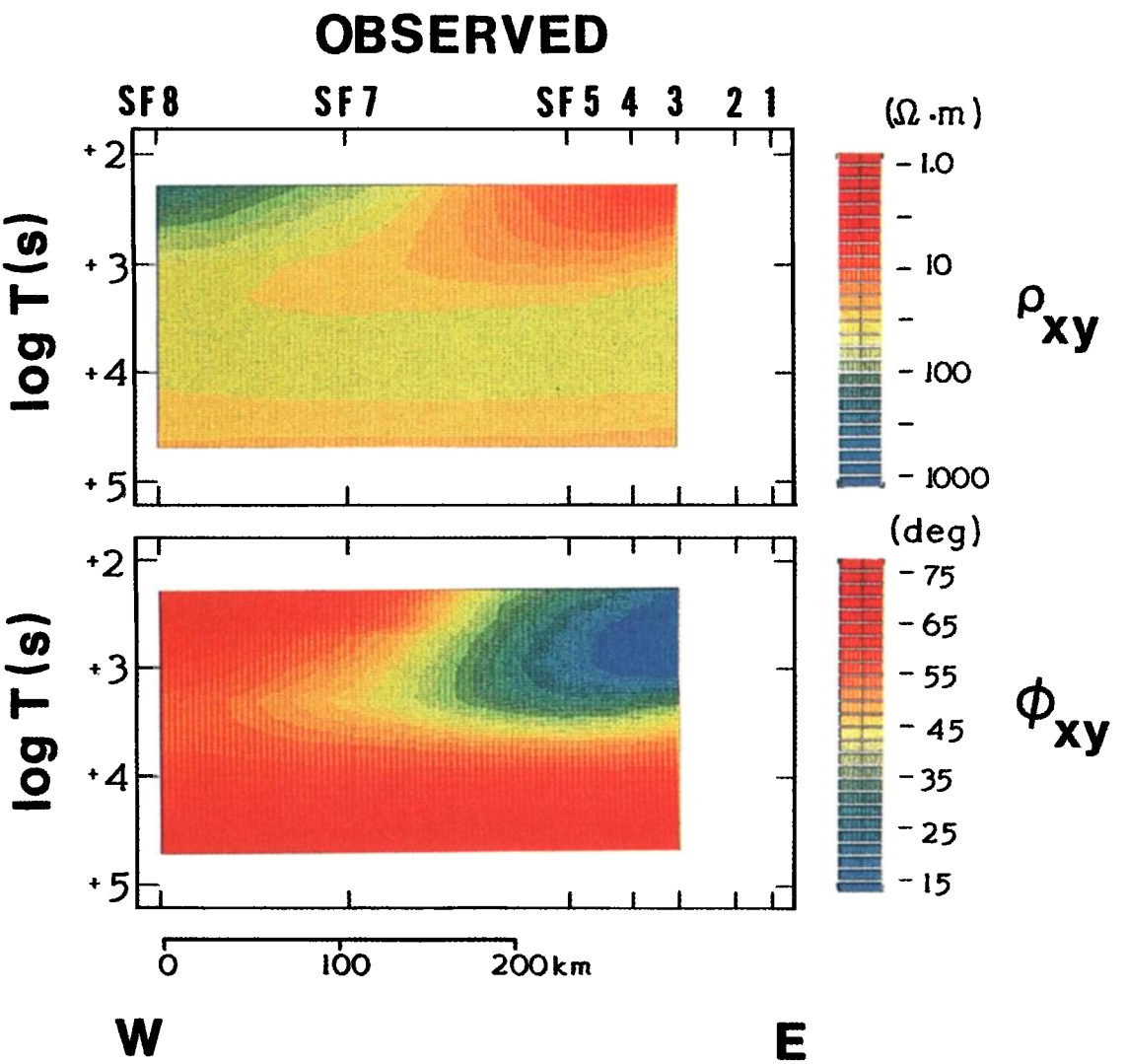

Plate 4. [*Wannamaker et al.*]. Pseudosections of transverse electric apparent resistivity ρ_{xy} and impedance phase ϕ_{xy} observed along the sea floor portion of the Lincoln Line. Note differences in horizontal scale and period range between land and sea floor results.

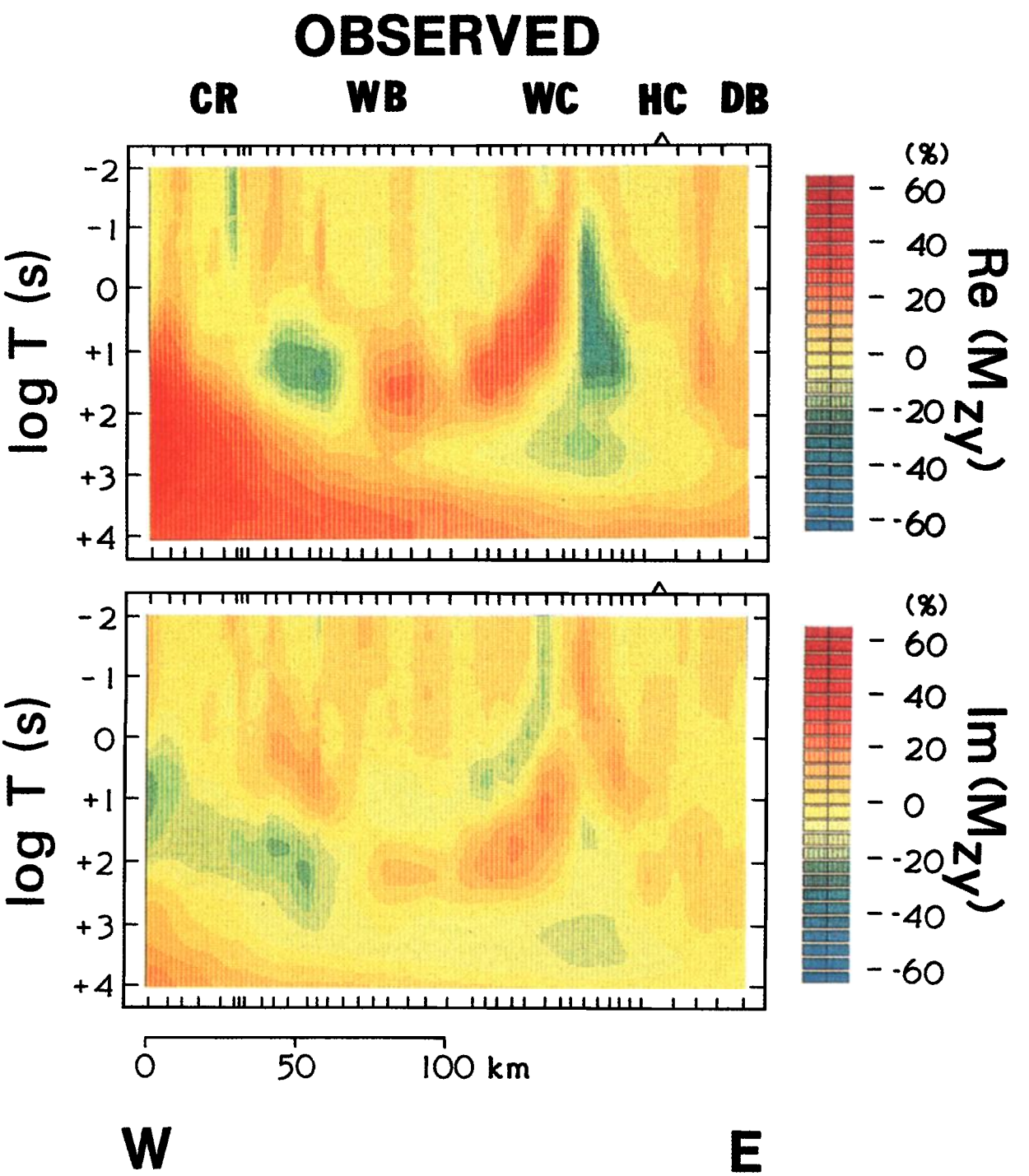

Plate 5. [*Wannamaker et al.*]. Pseudosections of vertical magnetic field transfer element M_{zy}, real and imaginary parts, observed along the landward portion of the Lincoln Line.

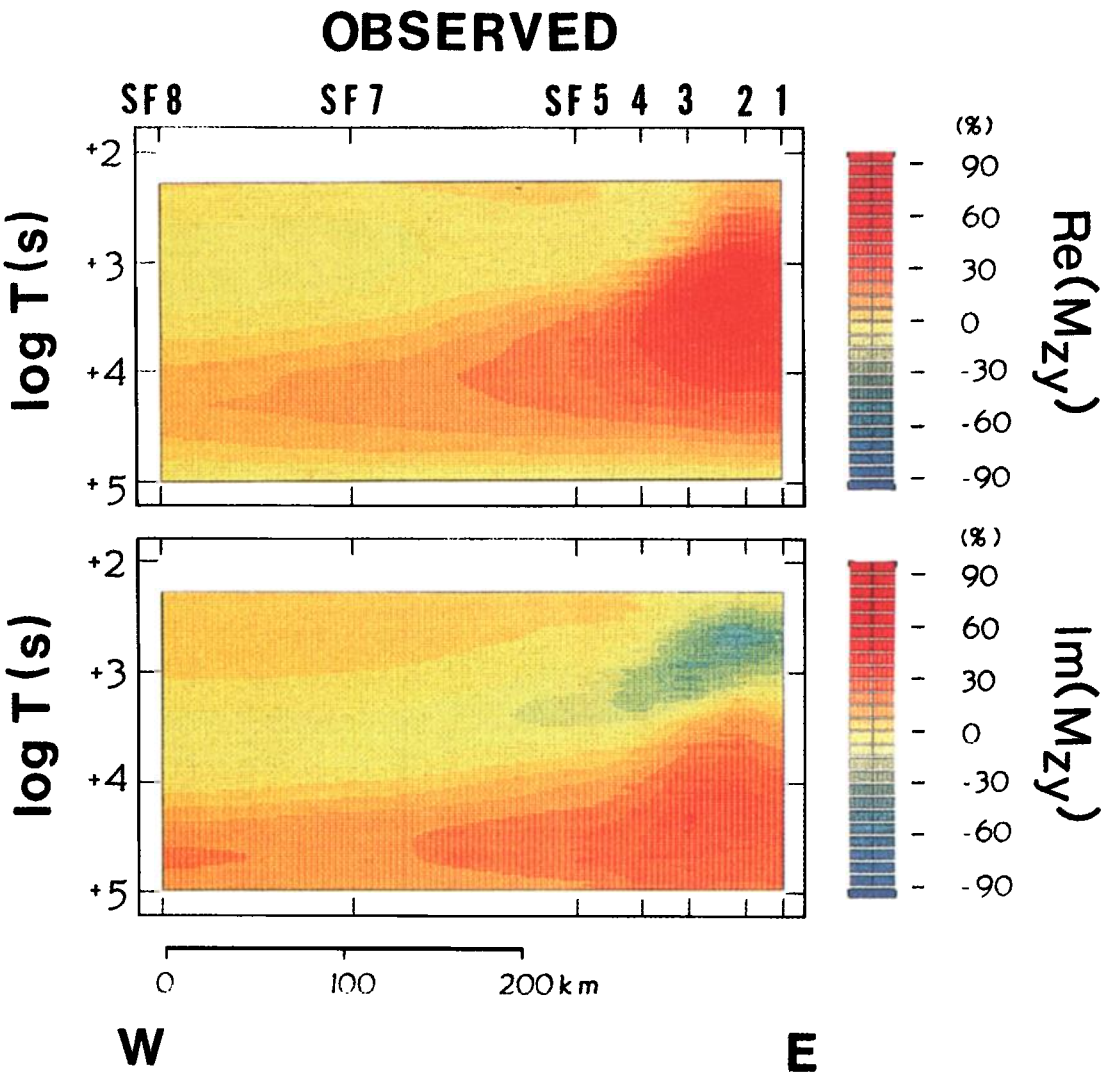

Plate 6. [*Wannamaker et al.*]. Pseudosections of vertical magnetic field transfer element M_{zy}, real and imaginary parts, observed along the sea floor portion of the Lincoln Line. Note differences in horizontal scale and period range between land and sea floor results.